AD-A189 846 FRACTURE TOUGHNESS TESTING OF A CERAMIC MATRIX COMPOSITE(U) AIR FORCE INST OF TECH WRIGHT-PATTERSON AFB OH SCHOOL OF ENGINEERING R P VOZZOLA DEC 87 1/2

UNCLASSIFIED AFIT/GAE/AA/87D-24 F/G 11/2 NL

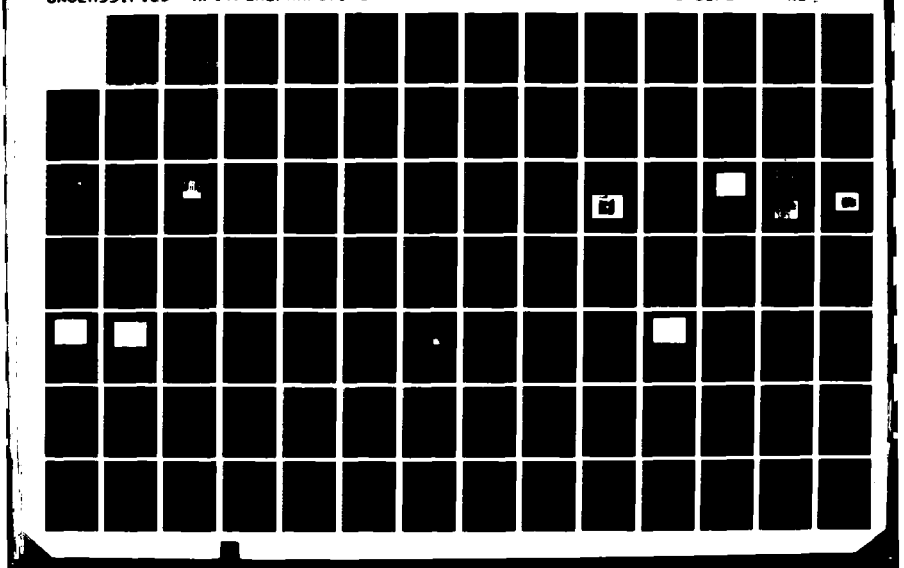

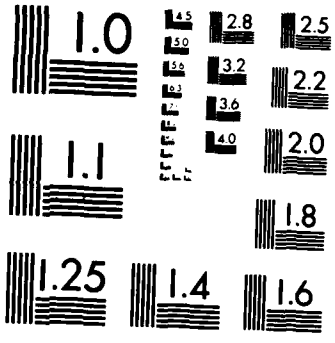

FRACTURE TOUGHNESS TESTING OF A CERAMIC MATRIX COMPOSITE

THESIS

Robert P. Vozzola
Captain, USAF

DEPARTMENT OF THE AIR FORCE
AIR UNIVERSITY
AIR FORCE INSTITUTE OF TECHNOLOGY

Wright-Patterson Air Force Base, Ohio

FRACTURE TOUGHNESS TESTING OF A CERAMIC MATRIX COMPOSITE

THESIS

Robert P. Vozzola
Captain, USAF

AFIT/GAE/AA/87D-24

Approved for public release, distribution unlimited

AFIT/GAE/AA/87D-24

FRACTURE TOUGHNESS TESTING OF A CERAMIC MATRIX COMPOSITE

THESIS

Presented to the Faculty of the School of Engineering
of the Air Force Institute of Technology
Air University
In Partial Fulfillment of the
Requirements for the Degree of
Master of Science

Robert P. Vozzola, B.S.
Captain, USAF

December 1987

Preface

The purpose of this study was to develop a technique for Mode II fracture testing of small composite specimens. The technique could be varied for uses with other fracture modes and for high temperature applications.

At this opportunity, I would like to express my gratitude to my thesis advisor, Dr. S. Mall for his advice and guidance.

I would like to extend a special thanks to Dr. T. Nicholas, of AFWAL/MLLN, and his staff of engineers. Larry P. Zawada provided extensive help with composite fabrication and post mortem analysis. Stephan Russ provided guidance on specimen preparation. Jay R. Jira's help was instrumental in getting the laser interferometry up and working.

I deeply thank my wife, Diane, for the typing, encouragement, patience and understanding she showed during the time of this study.

Robert P. Vozzola

Table of Contents

List of Figures

List of Tables

Abstract

The need for an accurate fracture toughness testing technique for fiber reinforced ceramic composites was identified. A technique was developed to measure small crack mouth displacements over small gauge lengths of small glass-ceramic composite specimens during loading. The technique was applied to Mode II crack propagation. A loading fixture capable of exerting and measuring small loads was developed. A technique to measure compliances in small composite specimens was perfected. The validity of using a laser based interferometric technique to determine the instant of crack initiation was studied. Finally, the Mode II critical strain energy release rate of interlaminar delamination growth was evaluated. Sample results for a 1723 glass matrix, silicon carbide fiber composite are included and recommendations for further study are described. (These).

I. INTRODUCTION

Problem

As new technologies push material usage closer to their physical limits, fracture mechanics has become an important tool in the design process. The durability of a part or structure is often directly related to a material's resistance to crack initiation and growth. By accurately predicting stable crack growth behavior, the usable life of a component can be assessed quantitatively. This aids the engineer in both his design selection and maintenance scheduling.

Griffith (1,2) provided the basic concepts of fracture mechanics in the 1920's and Irwin (3) and others followed on his work in the 1940's and 1950's. The early work was done with homogeneous isotropic materials, first with glass and then with metals (4). In recent years, composites have received an increasing amount of attention. Any analysis of composites is difficult due to their non-homogeneous and anisotropic nature (5).

With the high temperature requirement for new engines, new materials are needed. Researchers have sought to develop tough ceramics whose performance characteristics retain the best properties of their parent ceramics and have the additional quality of not being susceptible to fracture (6-9). The development of fiber

reinforced glass-ceramic matrix composites is one of the best examples in this direction.

Since the motivation for developing these ceramic composites is to utilize their high toughness in structural applications, an accurate fracture toughness measurement technique is needed. There is a standard procedure recommended by the American Society for Testing and Materials (ASTM) for finding the fracture toughness for metals at room temperature (10). No such procedure exists for fiber reinforced ceramic composites.

According to Jenkins (11), "Fracture testing of structural ceramics is complicated by the lack of an accurate technique for measuring the small crack opening displacement. This is further complicated by the small crack sizes which are associated with specimens at failure". Further, the composite specimens available for testing are small due to the limited availability of material. In addition, fracture testing at very high temperatures is required since these ceramic composites are being developed for high temperature applications.

Kobayashi and Jenkins were able to determine specimen compliance and fracture toughness parameters using a laser interferometric strain gauge (11,12). The laser interferometric strain gage (LISG) measures small displacements of the order of microns over small gauge lengths. Sharpe (13-16) was one of the pioneers in using

this technique for measuring crack surface displacements. In the past, this technique was primarily used with metallic specimens that had good reflecting surfaces. Due to the low reflectivity of most ceramic and glass composites, this technique has not been commonly used for these materials. To get around this problem, metal tabs have been glued onto the composites and the indents were placed on the tabs (12). The majority of this work has been applied to Mode I crack opening.

With composites, fracture due to crack growth in shear sliding Mode II or Mixed Mode I and II is of a potentially greater significance. This is particularly true with unidirectional fiber reinforced composites. The composite fibers serve as obstructions to Mode I fractures perpendicular to the fiber direction. However, cracks oriented parallel to the fibers can propagate and fail catastrophically in Mode II. To model the Mode II fracture, a three point bend configuration is used. The end-notch flexure (ENF) specimen has been successfully used to measure G_{IIc}, the critical strain energy release rate of interlaminar delamination growth in composites (17).

The flexure specimen is a beam with a crack located on the neutral plane at one end. The beam is subjected to three-point bending. Mall (18), used this type of beam when he investigated Mode II failure of composites using a finite element technique. Giare (19) measured Mode II

fracture toughness using a clip gauge to measure relative displacement of a crack surface on an end-notch flexure specimen. He was able to apply Linear Elastic Fracture Mechanics (LEFM) to a unidirectional glass fiber reinforced composite material in Mode II. A good technique is still needed that can accurately predict Mode II fracture at a wide range of operating temperatures.

Objective

The objective of this study was to develop a technique to measure small crack mouth displacements over a small gauge length of a small glass-ceramic composite specimen during loading. The technique was specifically applied to Mode II crack propagation. The utility of this technique was demonstrated for room temperature fracture testing of ceramic composites. A variation of the technique could also be used effectively at elevated temperatures in the future.

Approach

The experimental program involved several aspects. First, a loading fixture capable of exerting and measuring small loads was developed. Measurement of the load point displacements was also incoporated into the apparatus. Next, a technique to measure compliance in small composite specimens was perfected. Then a laser based interferometric technique was used to measure crack opening displacement and to determine the instant of crack initiation. Finally, the Mode II fracture of a

unidirectional glass matrix composite was investigated using the technique and hardware that was developed by using the end-notch flexure specimen.

The composite used was a 1723 Corning glass matrix with silicon carbon yarn as reinforcing fibers. This ceramic composite is currently being developed and studied by engineers at the Air Force Materials Laboratories. The results of this study provide an accurate experimental tool to perform fracture toughness testing of many structural composites in a variety of conditions.

II. BACKGROUND

Griffith developed one of the basic theories of fracture mechanics in the early 1920's (1,2). Griffith used brittle glasses to derive equations for crack propagation. His equations were based on the idea of critical energy release rate. He stated that "crack propagation will occur if the energy released upon the crack growth is sufficient to provide all the energy that is required for crack growth (4)".

The field of fracture mechanics took on greater importance in the 1940's and 1950's with the increased use of high strength materials. Irwin (3) applied fracture mechanics to metals. He did extensive studies on the effects of stress on the crack tip and the crack tip plastic zone size. Broek (4) presents a good history of the basic problems and concepts of Linear Elastic Fracture Mechanics in his book. The bulk of these works, however, deal with homogeneous isotropic materials such as metals and simple glasses.

Composites are non-homogeneous and anisotropic in nature. This complicates any analysis of composite materials. The basic mechanics of composite materials are described by Jones (5). Many of the new composites are being developed for high temperature applications in today's engines.

One of the areas of study for these applications is tough ceramic composites. The toughening mechanisms for ceramic composites were described by Jelinek (20). Jelinek lists three methods of toughening ceramic composites: 1) increase the local driving force necessary to propagate cracks to failure, 2) locally increase the mechanical energy consumed per unit area of propagation of any crack, or 3) decrease the local strain by cracking, which reduces the stress concentration. Jelinek also lists six ceramic matrix composite toughening concepts.

The Ceramic Bulletin (21), provided information on processing techniques for fiber-reinforced ceramic matrix composites. The article deals with properties and processing of several composites, but concentrates mainly on silicon carbide reinforced glasses and composites. The article discusses processing from the initial slurry, through hot pressing and includes information on future needs and directions.

The Naval Research Laboratory has done work on refractory-ceramic fiber composites (22). The engineers at the Research Laboratory present the significant opportunities, problems, and possible solutions associated with ceramic fiber composites. Processing, mechanical properties and limitations of the composites were all discussed.

Hasselman (23-25), did extensive work in ceramic composites. His works concentrated in the areas of thermal shock and thermal stress fracture. He stated that tailoring of material properties could be achieved to improve resistance to fracture initiation and resistance to crack propagation. This was achieved by adding substances to the matrix of a composite.

Kelly (26), used Hasselman's theories to study the influence of the addition of silicon carbide whiskers and zirconia on the material properties of a parent ceramic. Valentine (27), also followed some of Hasselman's techniques in the study of strength and thermal shock behavior of a ceramic composite. Valentine compared results based on varying compositions of a particulate and varying temperatures up to 1500°C. Both Kelly and Valentine characterized the microstructures of the composites that resulted from their experimentation.

One of the acknowledged experts in the area of glass-ceramic matrix composites is Dr. Karl Prewo. He has done extensive research at the United Technologies Research Center and he has published numerous articles on reinforced glass matrix composites and glass ceramic matrix composites (7-9, 28-36).

Prewo has completed a series of reports for the National Aeronautics and Space Administration on Research on Graphite Reinforced Glass Matrix Composites. In these reports Prewo describes composite fabrication procedures,

composite characterization procedures, and the results and discussion of those procedures.

Prewo described three point flexural strength, creep and fatigue tests for several glasses, including aluminosilicate glass composites. He found that the glass and glass-ceramic matrix composites to show great promise for high temperature applications. He did not, however, do any Mode II testing with end-notch flexure specimens.

Prewo did a range of tests and property studies at high temperatures up to about 1000°C. He noted, "The predominant mode of failure from room temperature to 600°C is local delamination of the composite along the fiber direction, indicative of a weak bond at the fiber matrix interface" (33).

Additional fabrication information was provided by Mr. Larry Zawada of AFWAL/MLLN (37). Mr. Zawada has been experimentally preparing small samples of the 1723 glass matrix composite. He has also been involved with mechanical property testing of this ceramic composite.

There are several sources which deal with fracture toughness testing. The American Society for Testing and Materials (ASTM), has several sources for metallic materials (10,38). ASTM also published guidelines for flexural tests of plastics and electrical insulating Materials (39).

Kobayashi has detailed experimental techniques in fracture mechanics (40, 41). He describes compliance measurements, testing systems and instrumentation, mixed-mode stress intensity factors, laser interferometry and many other fracture mechanics testing techniques.

Kobayashi also served as an advisor to a doctoral student, M.G. Jenkins. The two collaborated on several articles and a dissertation on short crack growth of ceramic composites (11,12,42,43). Jenkins and Kobayashi performed Mode I tensile testing on a number of metals and ceramics. The result of their study was the development of a technique for fracture toughness testing of ceramics. Jenkins used a laser interferometric strain gauge to measure crack mouth opening displacements at high temperatures. He perfected a technique of indenting small metal tabs that were affixed to the ceramic specimens. He was able to measure compliance, work of fracture, and crack mouth opening displacement. The compliance was used to calculate an effective crack length and the crack growth resistance. This led to determinations of the stress intensity factor K_I, and the strain energy release rate G_I.

The laser interferometric strain gauge was extensively tested by Sharpe (13-16, 44-48). For the past twenty years Sharpe has used laser interferometry for various applications of displacement measurement. He has used a metal tabbing technique for room temperature

testing of graphite-epoxy components. He did preliminary work on the applicability of the measurement of displacements parallel to a crack in a composite specimen. Sharpe found that the LISG measurements parallel to the crack were crude and only approximate. Sharpe also did high temperature work on displacements over short-gauge lengths. The majority of Sharpe's testing concerned fatigue crack growth.

Locally, Bar-Tikva used laser interferometry in his thesis work on an experimental weight function method for stress intensity factor calibration (49). Bar-Tikva used the LISG to find stress intensity factors of four-point bend specimens. A computer program was then used to construct a weight function. Bar-Tikva (50), combined with Grandt and Palazotto in a presentation of the results and conclusions that were drawn from the previous work on the weight function.

Mr. Jay Jira, an engineer of the Metals and Ceramics Division, AFWAL/MLLN, completed a computer program to record and process the fringe input from the laser interferometric strain gauge (51). His work is on-going in this field in the area of fatigue crack growth in metals. Jira's program was originally intended for Mode I fracture.

The majority of the laser interferometric work has been with isotropic materials. It has been proven very reliable for measuring small displacements in these

materials. The use of the LISG with composites, especially in Mode II fracture, is fairly new.

According to Jones (5), the effect of a transverse shear may be more important for laminated composites than for isotropic materials. This view is strongly supported by Giare (19). Giare studied Mode II failure of reinforced composites. He used clip gauges to measure the crack mouth opening displacements versus load. These measurements led to the measurement of critical Mode II stress intensity factor. Giare showed that the crack growth resistance curve is a material property and that linear elastic fracture mechanics applies well to unidirectional glass fiber reinforced composite materials in Mode II fracture.

Mall (18), applied a finite element analysis to an end-notch flexure specimen in Mode II. He investigated the effects of overhang on the Mode II strain energy release rate.

Finally, once all the testing has been completed the fractures must be examined and understood. Wiederhom (52) investigated brittle fracture in ceramics. He stated that the fracture behavior of metals and ceramics were different. Fracture in ceramics was controlled by the microstructure on the crack tip. Lankford (53) completed a report on damage mechanisms in ceramic composites. Lankford tested glass-ceramic matrix composites reinforced with silicon carbide fiber. He tested unidirectional and multiaxial reinforced composites in compression. His

damage characterization goes to the microscopic level. Marshall (54) studied failures during both tensile and flexural loading.

III. EXPERIMENTAL PROCEDURE

The experimental procedure involved fracture testing of straight-notched, pre-cracked, end-notch flexure specimens of unidirectional fiber reinforced beams at room temperature. The beam was composed of 1723 Corning glass matrix (see Table I) with a silicon carbide yarn fiber (see Table II). Appendix A describes composite fabrication and shows a photograph of the ceramic composite's fiber and matrix. A linear variable displacement transducer (LVDT) and loadcell were used to monitor the load vs. load point displacement during load application and subsequent fracture. The resulting load vs. displacement curves were used to calculate compliance vs. crack length curves. The laser interferometric strain gauge was used to monitor crack opening displacement. The values of displacement vs. load were used to determine the critical load accurately. The specimen geometries, pre-cracking, loading apparatus, compliance technique, laser interferometric strain gauge, reflective tabs and output are discussed separately in the following sections.

Specimen Preparation

An end-notch flexure specimen was used in this study. The overall dimensions of the beam were 2.0 x 0.30 x 0.20 inches, with a notch width of approximately 0.010 to 0.015 inches, and a testing span of 1.50 inches. The dimensions of each specimen were measured with a micrometer and were

TABLE I

Properties of Corning 1723 Glass

Constituents	Nominal Composition (Wt.%)
SiO_2	56.8
B_2O_3	4.3
Al_2O_3	15.5
CaO	10.0
BaO	6.0
MgO	6.9
As_2O_3	0.5
Strain point (°C)	665
Annealing point (°C)	710
Softening point (°C)	908
Working point (°C)	1168
Melting point (°C)	1550

Table II (34)

Materials Used to Reinforce Glass and Glass-Ceramic Matrices

Material	Diameter (μm)	Density (g/cm)	E (GPa)	Ultimate tensile strength (GPa)	Thermal expansion coeffic. (10^{-6}/°C)
Boron mono-filament	100-200	2.5	400	2.75	4.7
Silicon carbide mono-filament	140	3.3	425	3.45	4.4
Carbon yarn	7-10	1.7-2.0	200-700	1.4-5.5	-0.4 to -1.8
Silicon carbide yarn*	10-15	2.55	190	2.4	3.1
FP alumina yarn**	20	3.9	380	1.4	5.7
Alumino-boro-silicate yarn+	10	2.5	150	1.7	
VLS-SiC whisker++	6	3.3	580	8.4	

*Nicalon, Nippon Carbon Co. Tokyo, Japan
**E.I. Du Pont de Nemours & Co., Inc. Wilmington, DE
+Nextel 312, 3M Co., St. Paul, MN
++Los Alamos National Lab, Los Alamos, NM

all within two percent of the stated values. Figure 1 defines the dimensions for the specimen. The machined notch length varied from 0.1 to 0.2 inches and was followed by various lengths of precracking. The beam thickness corresponded to a forty ply lay-up of the glass composite. The material fabrication is explained in appendix A. The beam width was chosen from previous experiences with this composite by engineers in the Air Force Materials Laboratory.

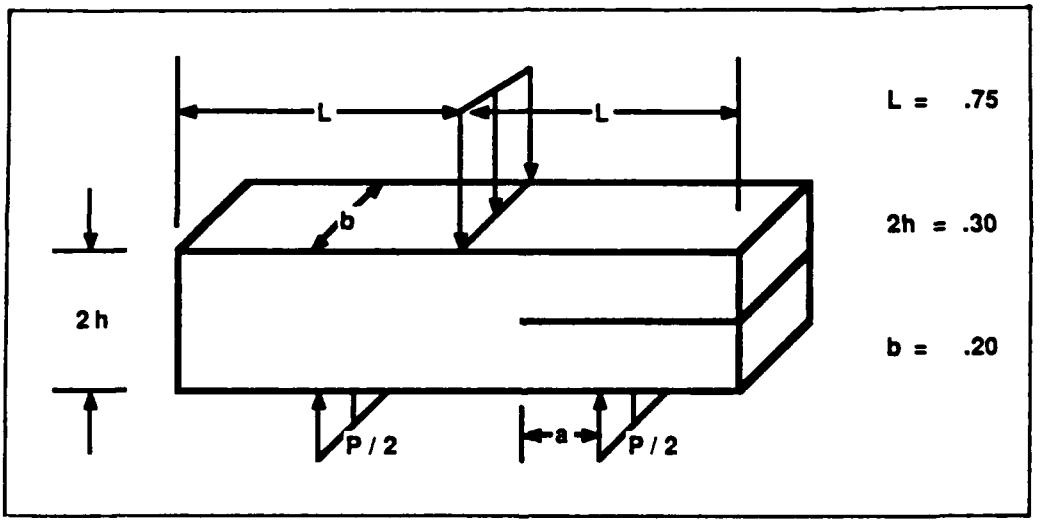

Figure 1. Specimen Dimensions

The notches were cut using a liquid cooled diamond wheel saw. The resulting notch widths were 0.010 to 0.015 inches. The notches were cut at the edge of the beam at half of the height. This would correspond to the location

of the beam's neutral plane. The fibers run parallel to this plane and notch.

Pre-cracking

In order to create the natural crack front for accurate fracture toughness measurement, the machined notch was extended by precracking it before conducting actual tests. A white paint was applied on one side of the specimen from the notch to the back edge. The white paint allowed for easier monitoring of crack growth on the black fibrous composite. A straight razor was used to cut a sharp crack in the center of the blunt notch tip. After the desired crack length was decided and the location marked with a thin pencil, a transverse load was applied at this point. The compressive load was applied by using a small one inch metal C-clamp. To ensure that the transverse load was applied at the desired point, two one-quarter inch wide strips of metal were precisely positioned between the sides of ceramic specimen and the C-clamp (see Figure 2). The strips ran from the rear of the specimen to the point where the crack was intended to arrest. The strips were used to more evenly distribute the load from the C-clamp and the create a track for the possible movement of the load location. For all practical purposes, the pre-crack was arrested at the desired point.

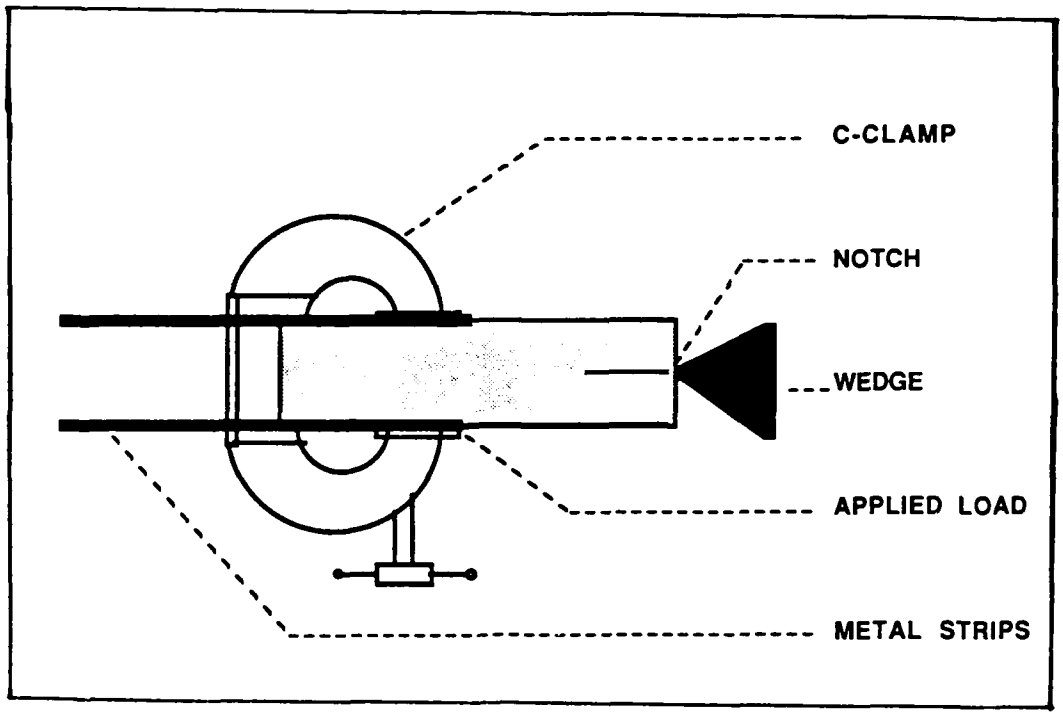

Figure 2. Pre-crack Configuration

The C-clamp holding the specimen was then mounted in a vise, which was attached to a workbench. A travelling microscope was positioned to view the crack tip. For best results, the specimen face should be parallel to the travel of the ten power microscope. In this way, it is easy to follow the crack as it propagates to the desired point.

A small screwdriver was then inserted in the notch and gently tapped with a hammer. This wedge action caused the crack to slowly propagate until it reached the area of the applied load. By watching the crack growth in a microscope the exact point of the crack tip could be determined and marked with a thin pencil. The overall crack length

was then measured and recorded for each specimen. These were also verified later on by the post-mortem examination of the fractured surfaces after conducting the fracture toughness test. This is described in the results section to follow.

Loading Apparatus

A custom-made loading apparatus was fabricated for the present study. It consisted of a rigid steel frame enclosing a moving platform. The platform is manually raised and lowered by a screwjack mounted to the bottom of the frame (see Figures 3. & 4.).

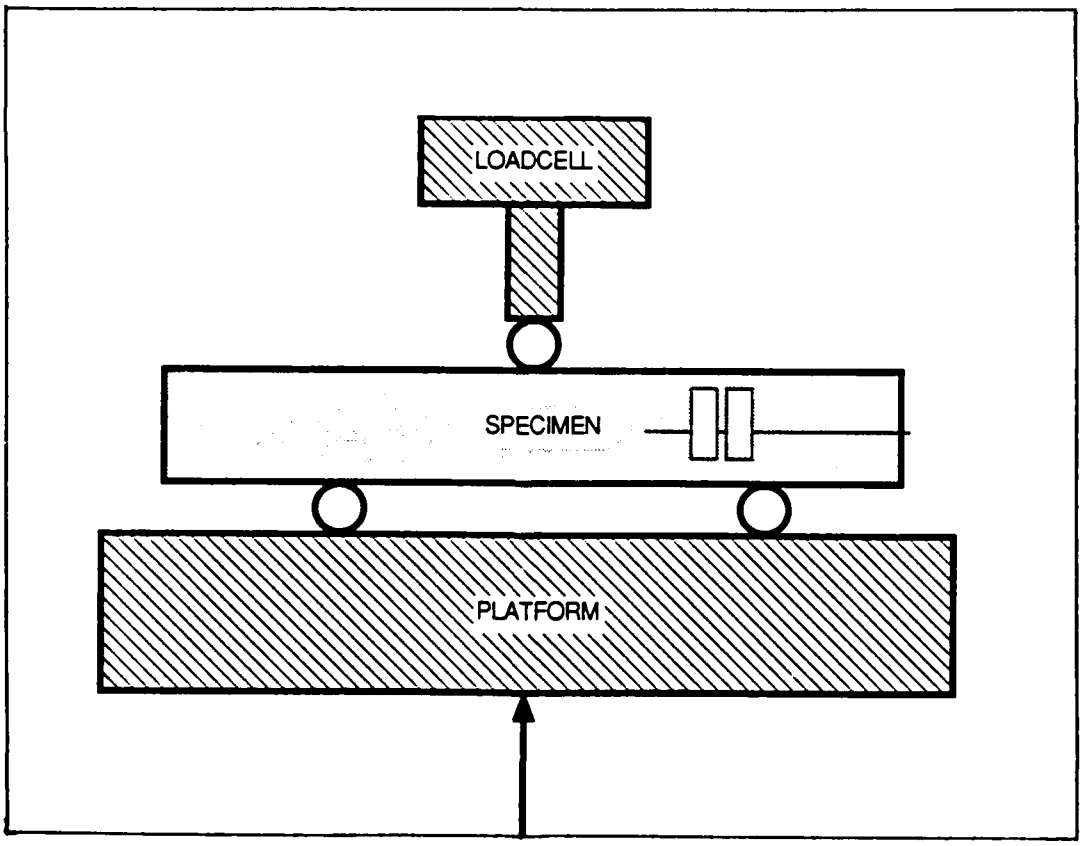

Figure 3. Three-Point Bend Platform

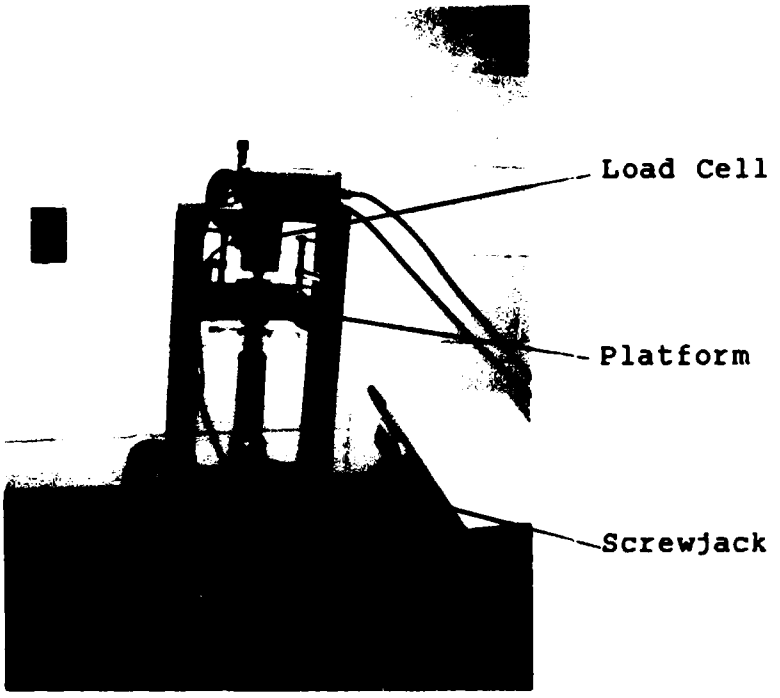

Figure 4. Loading Apparatus

The platform uses bearing sleeves and guide rods to stabilize vertical travel. Attached to the moving platform is a three-point bend configuration with the two lower rollers set 1.5 inches apart. The top roller is glued to a threaded stud attached to a load cell. The load cell is an Interface Model SM-1000 with a range of 1000 lbs. The load is applied by raising the stage to the load cell using a manually operated screwjack. The stage displacement and load point displacement are monitored by a LVDT. The LVDT is a Robinson-Halpern Model 225A-125 which has a range of

± 0.125 inches and an output of up to 2.19 volts at maximum range.

The outputs from the LVDT and load cell are fed to a two-channel Hewlett Packard X-Y Plotter. The resulting plots of load vs. load point displacement can be used to find the specimen compliance. The LVDT was calibrated to an accuracy of a thousandth of an inch and the load cell was calibrated to a pound.

Compliance Measurement

Based on preliminary testing on some thin composite specimens that were made previously, the approximate critical load was established for the tested specimen configuration. By staying well below that load, the load vs. displacement curves showed a linear relationship. Using the equation:

$$C = v/P \qquad (1)$$

where

C = compliance

v = load point displacement

P = applied load

The compliance was calculated for different crack lengths from several identical specimens. Effective crack lengths were varied by testing specimens of varying initial crack

lengths by moving the specimens on the bottom rollers (see Figure 3.). According to Mall (18), the overhang portion of a beam has no effect on the evaluation of G_{II}. This technique allowed the testing of several effective crack lengths on each specimen. To ensure minimum errors in experimentation, each crack length was tested three times and the compliance value was then averaged over the three. Finally, to minimize the friction forces and closure between crack faces, 0.012 inch metal rollers were inserted in the notches during this measurement process. Mall (18) suggested this technique to negate the undesirable effects of friction in the region above the support pin.

Each beam was inserted on the three point bend platform and carefully placed perpendicular to the upper loading pin. The specimen was then moved parallel to a fine graduated metal rule attached to the platform. The overhang portion of the beam was then measured. The overhang portion is the length of beam from the point above the lower support pin to the end of the specimen. Mall (18) proved that only the area between the two lower support pins effect the evaluation of G_{IIc}. The amount of overhang was then subtracted from the actual crack length to provide an accurate measurement of effective crack length.

The three-point bend platform was then raised until the specimen was just below the upper loading pin but still not touching. The Y-axis was set to zero on the X-Y plotter. This gave the reference value for zero load.

Returning to the loading apparatus, the platform was then raised until it touched the loading pin and a small load was applied. The output of the LVDT was then checked with a multimeter to insure that the readings were in the linear range of the LVDT. If the readings were outside the linear range, the LVDT was adjusted accordingly. Once the LVDT was properly aligned, the X-axis (the displacement axis) of the X-Y Plotter was set to zero and the pen was set to record.

The load was then applied until a previously determined displacement was achieved. The displacement corresponded to an approximate load that was well below the expected critical load. At the end of loading the pen was raised on the plotter and then the specimen was unloaded. This cycle was completed three times before the specimen was moved slightly and another effective crack length was tested.

Finally, several specimens were run at various effective crack lengths. This provided load vs. load point displacement readings for effective crack lengths from zero to half span of the beam. This also gave overlapping values of readings from the different specimens. The compliance was then calculated using the equation $C = v/P$.

After all the compliance curves were generated, a crack length was chosen and the specimen was loaded until shear failure occurred. The crack propagated towards the center of the loading span. This process was recorded on the X-Y plotter in the same manner as the compliance measurements. It was during this phase that the laser interferometric strain gauge was required to determine the actual measurement of critical load at crack initiation.

Laser Interferometric Strain Gauge

The Laser Interferometric Strain Gauge (LISG) was used by Sharpe (15) to measure displacements of less than a micron. The LISG measures the relative displacement of two small reference marks. The reference marks are made by using a diamond micro-hardness indenter. The indenter makes square based pyramids whose size is based on the load used on the indenter and the material being indented. Sizes of indents range from 20 microns to over 100 microns. Spacings between indents range from 50 microns to 800 microns based on the application (Ref. 15, 19, 20).

A laser acts as a coherent light source to illuminate the indentations. The beam is reflected at an angle α off the indentation faces. The reflected light from the two closely placed indentations overlaps and forms a interference fringe pattern on both sides of the incident laser beam.

The application of load causes the specimen to deform and the indents to move relative to each other. The motion of the indent spacing and the fringe order is related by the equation:

$$\delta d = \delta m \lambda / \sin \alpha \qquad (2)$$

where

δd = change in distance between indentations

λ = wave length of the light source

δm = change in fringe order

α = laser incidence angle

The wavelength of the helium-neon laser is 0.633 microns. The laser incidence angle is approximately 44 degrees, which is related to the geometry of the indentations. The indent spacing was 300 microns prior to loading.

Photo detectors are placed at fixed points to monitor the fringe patterns and count the number of fringes passing. By using a photo detector on each side of the incident beam, the rigid body motion can be eliminated. This is done by averaging the left and right fringe number.

Since the glass composite in this study was not very reflective, tabs are required for employing the laser interferometric technique.

Reflective Tabs

Two thin metallic tabs were attached to each specimen. The tabs were laid across the pre-crack and epoxied at two corners, diagonally across from each other (see Figure 5). The two independent tabs were then indented. The method of epoxying the tabs caused one tab to move with the upper shear surface and the other tab to move with the lower shear surface. The indents moved away from each other horizontally. The movement of these reflective indents was the quantity measured using the LISG.

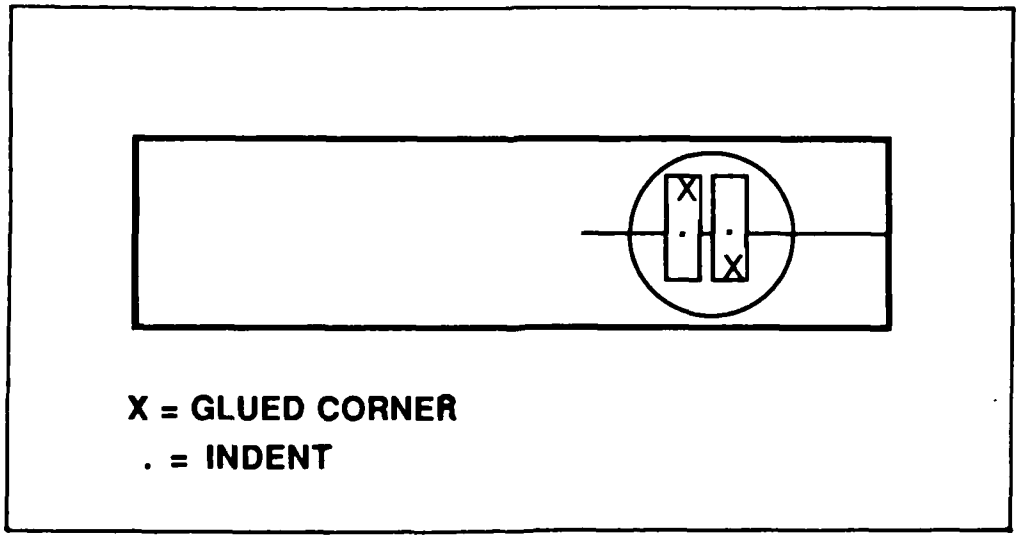

Figure 5. Tabbing Method

The reflective tabs were cut from a 0.004 inch thick sheet of aluminum. Aluminum is highly reflective and is also pliable enough to provide good indents and ease of preparation at room temperature. At higher temperatures, platinum tabs have been used (12).

Using a razor, a rectangular piece of aluminum, approximately 0.2 x 0.1 inches was cut from the sheet. The top of the rectangular piece was then marked. Using a hammer blow to a straight razor, this piece was cut in two halves parallel to the long side. Figure 5 shows the two tabs schematically, while Figure 6 shows a photograph of the highlighted area.

Figure 6. Reflective Tabs

Magnified X25

A 2.0 x 0.1 inch piece of cellophane tape was placed on the shiny side of one of the tabs. The tape was rolled back and epoxy was applied to the bottom of the tab. After the tape was aligned, the tab was carefully placed near the crack tip and the epoxy was pressed away from the crack. The tape applied the needed pressure and the epoxy was left to cure for two hours. The tape was then removed. The second tab was carefully positioned on the composite next to the first tab. The lower portions of the two tabs were taped to the specimen. The exposed end of the first tab was slightly curled up to separate it from the second tab. The exposed end of the second tab was then carefully epoxied. The second tab was taped to the specimen and left to cure for two hours. After the epoxy had cured, all the cellophane tape was removed. The tabs were then ready to indent.

The two indents were generated using a 300 gram load on a Wilson hardness tester and a pyramid shaped diamond microhardness indenter. The resulting indents were approximately 130 microns on a side and were spaced approximately 300 microns apart using a precision stage and microscope (see Figure 7).

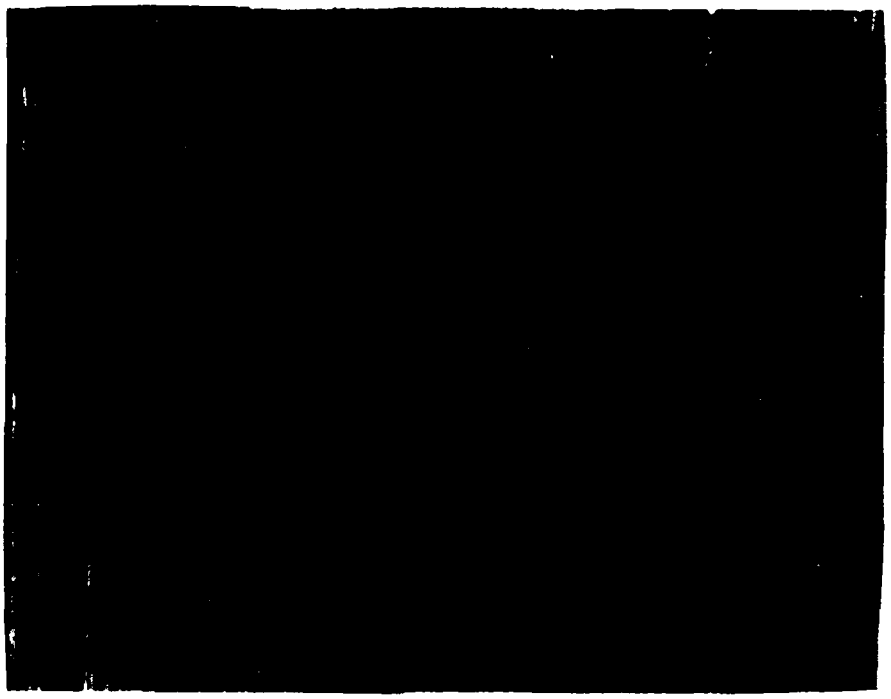

Figure 7. Reflective Tabs and Indents
Magnified 200X

The resulting indent planes were angled at approximately 45 degrees to the incident laser beam when the specimen was perpendicular to the loading pin. The two indents were illuminated by a coherent laser beam from a 10 milliwatt Helium-Neon laser (see Figures 8 and 9). The two over-lapping reflections produced interference fringe patterns at four locations located at 45 degrees relative to the beam. Only the two reflections at the sides are important for horizontal motion.

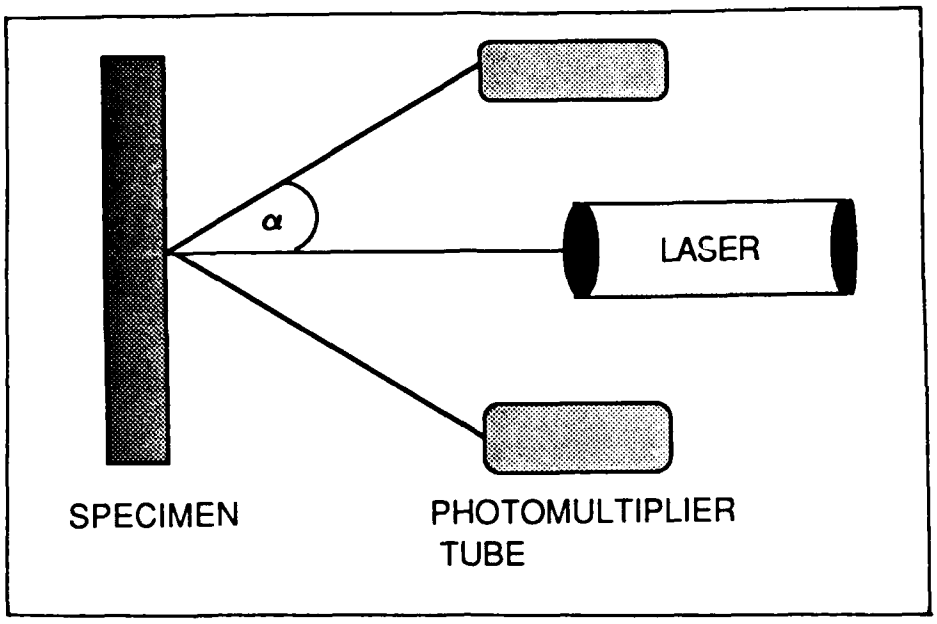

Figure 8. Schematic LISG Arrangement

Figure 9. Actual LISG Arrangement

The fringe patterns (see Figure 10), were reflected onto two photomultiplier tubes located 22 inches from the specimen. The active face of the photomultipliers was covered by a narrow slit 5 millimeters high, smaller than 1 fringe in size. The slit allowed distinction between individual fringes. The use of two photomultipliers negated rigid body motion by using an average value of displacement between the two readers. An isolation table provide adequate isolation from random vibrations of the surroundings.

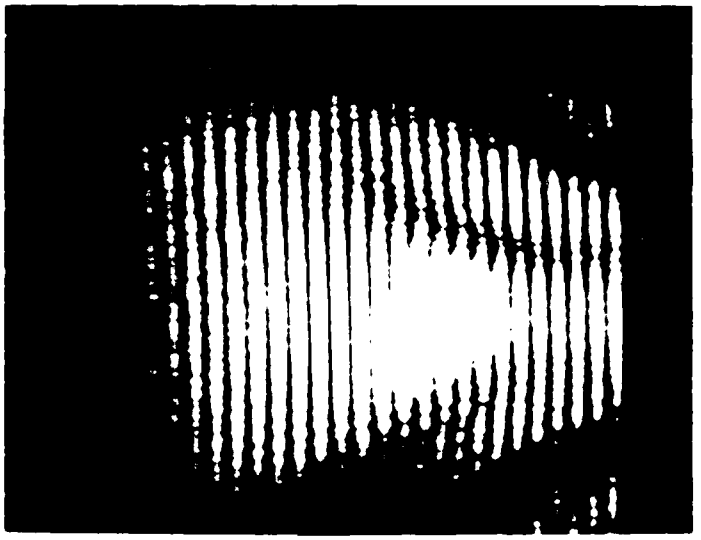

Figure 10. Fringe Pattern Reflections

Using equation (2), the displacement between the two indents near the crack surfaces was found as a function of applied load. This allowed for determination of the critical load. The fringe information and load were input to a Tektronix 4052 computer system through A/D converters. The fringe information was used to determine the relative displacement between the locations of the two indents. The displacement was looked at in a qualitative manner to determine the instant that the two crack facet moved in shear. During the shearing process the relative displacements changed abruptly from a stable linear load-displacement relationship to a non-linear relationship. The load at the point of change was identified as the critical load.

RESULTS AND DISCUSSION

Compliance

Seven of the end-notched flexure specimens were tested to generate a crack-compliance relationship which is required for G_{IIc} as discussed later. Each specimen was tested at several effective crack lengths by moving it horizontally across the two lower roller supports. It was very important to test each specimen as many times as possible due to the limited availability of materials. This technique provided multiple compliance readings for crack lengths ranging from 0.0 inches to midspan at 0.75 inches. The compliance was found using equation (1).

Since the specimen height varied slightly among the specimens (see Table III), the compliances were normalized by the cube of the height. The normalized compliances are plotted as a function of crack length in Figure 11. The results show the expected trend of the compliance increasing with crack length. Using the regression analysis, a curve was fitted to the experimental data. This is shown as a solid line in Figure 11 and is given as follows:

$$C = 1.646656 * \exp(0.506834)a/W \qquad (3)$$

where

a = the crack length from the support pin

W = L, the width of a half span

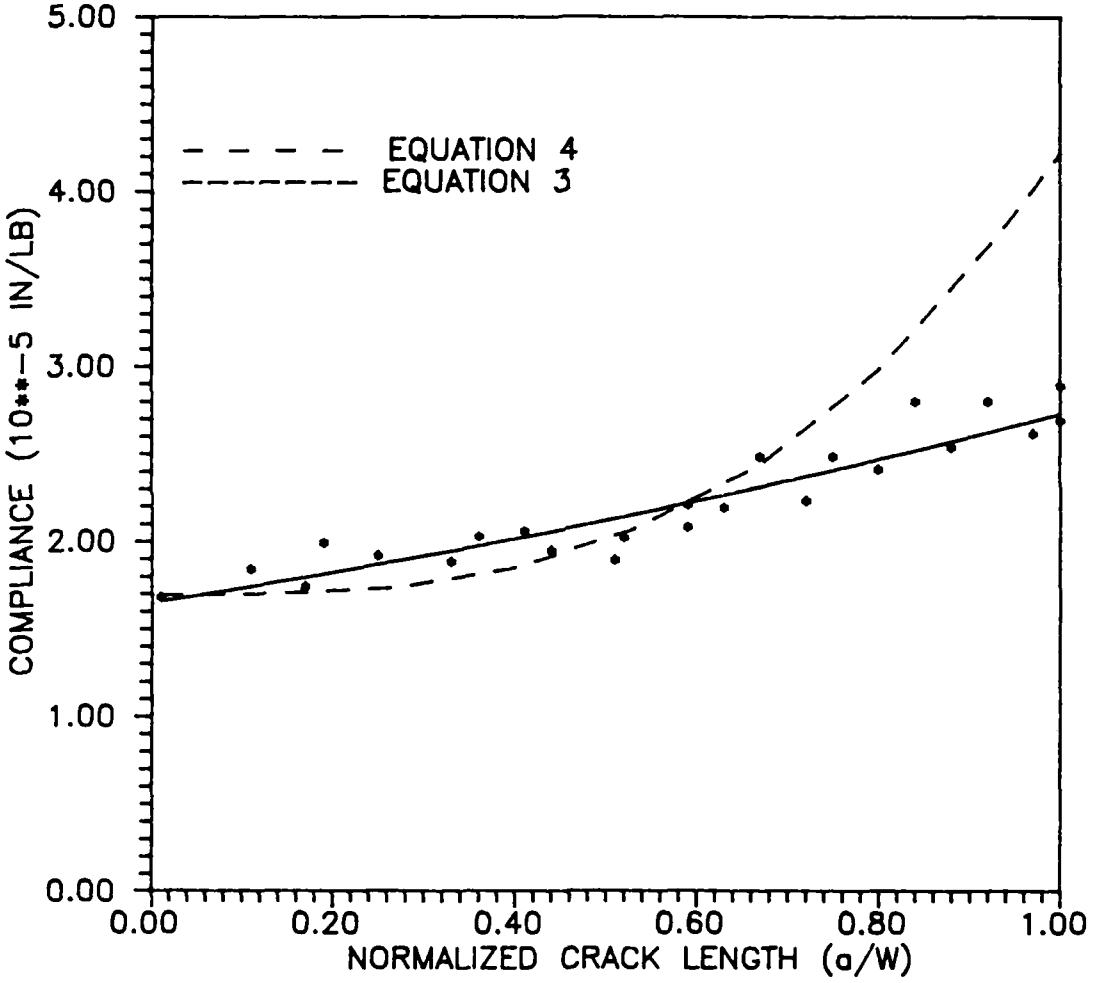

Figure 11. Experimental and Analytical Compliance Curves

Table III. Specimen Dimensions

Specimen Number	Overall Length (inches)	Height 2h (inches)	Thickness b (inches)	Half Span L (inches)
T-11	1.984	.306	.202	.75
T-12	1.992	.295	.201	.75
T-13	1.984	.298	.201	.75
T-15	1.984	.300	.200	.75
T-16	1.992	.298	.198	.75
T-21	1.984	.305	.203	.75
T-24	1.953	.303	.199	.75

As mentioned previously, the end-notched flexure specimen has been employed extensively to measure Mode II interlaminar fracture toughness, G_{IIc} in composites. A theoretical compliance relation has been developed by Russell (17) which is given below:

$$C = \frac{1 + 1.5(a/L)^3}{4E_{11}b(h/L)^3} \qquad (4)$$

This analytical relation was developed based on the simple linear beam theory. The present measured compliances were compared with the theoretical relation given in equation (4). This is also shown in Figure 11.

All variables in the theoretical compliance expression are known except for E_{11}. Young's Modulus, E_{11}, was calculated from equation (4) by using the experimental compliance for a crack length of zero. The calculated value of Young's Modulus was found to be 9.257×10^6 pounds per square inch.

The experimental and theoretical compliance relations are in reasonable agreement with each other up to a/W = .70, but they quickly diverged after that. This difference can be attributed to several factors, for example, the small size of the specimen or the simple beam theory. The nature of the small size of the fibrous composite provided much higher compliances at midspan in the analytical representation than in the experimentation. A more appropriate analytical model needs to be found for use with the small composite specimens.

Fracture Toughness

As stated, the objective of this study was to develop a procedure, as well as to measure, the critical strain energy release rate, G_{IIc}, for a fiber reinforced ceramic composite. Several specimens of the 1723 Glass matrix/silicon carbide fiber composite were tested until fracture. A typical load-displacement curve is shown in Figure 12.

All of the load-displacement curves are characterized by an initial section of linearity. The linear portion

extends past two hundred pounds of applied load. This portion of the curve corresponds to the elastic deformation of the beam.

The linear portion of the curve was followed by a nonlinear portion until the load ultimately dropped off as a result of fiber failure. Based on observations during testing, it was thought that the nonlinearity was a result of shear failure along the neutral plane.

The critical load is required to find G_{II}. Although shear fracture was evident during the nonlinear portion of the load-displacement plot, it was not possible to visually observe the instant of fracture initiation. Since visual observation could not back up our theory that fracture initiation occurred at the point of nonlinearity, the laser interferometric strain gauge was employed.

The laser was aligned so that the reflections from the two indents formed strong fringe patterns at angles of 45 degrees to the specimen surface. The photomultiplier tubes were then positioned in the center of each fringe pattern.

During loading, information from the photomultiplier tubes and the load cell was input to the computer once every second. The voltage from the photomultipliers showed steadily increasing or decreasing strength. By noting the local high and low points, the relative displacement was measured to half a fringe.

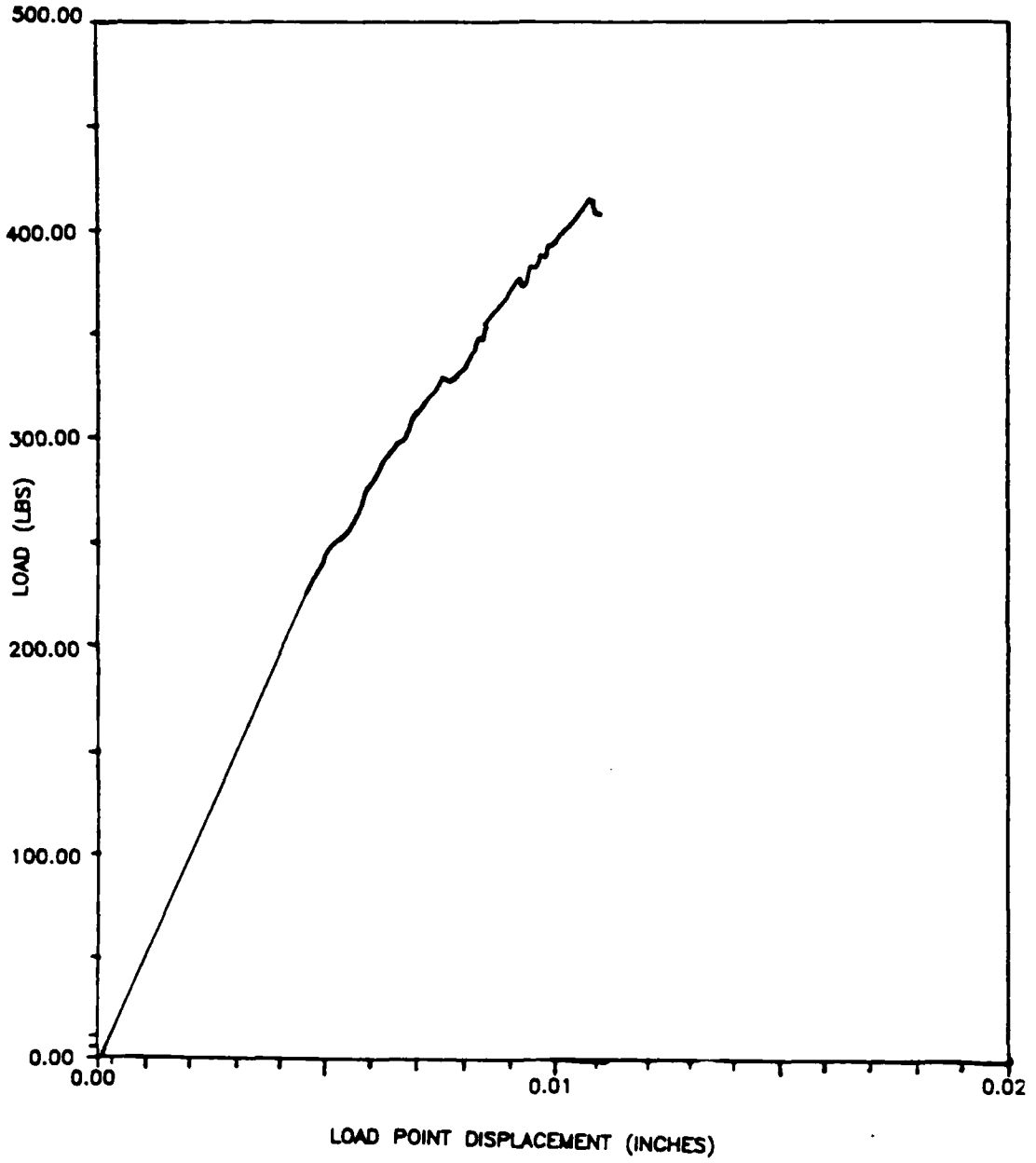

Figure 12. Loading to Fracture

During the loading process, the specimen provided a strong fringe pattern until a point when the patterns suddenly visibly degraded (see Figure 13). The loading process was continued and the LISG still recorded fringe information. The fringe intensity, however, had faded. The rate of fringe movement also increased rapidly at the point.

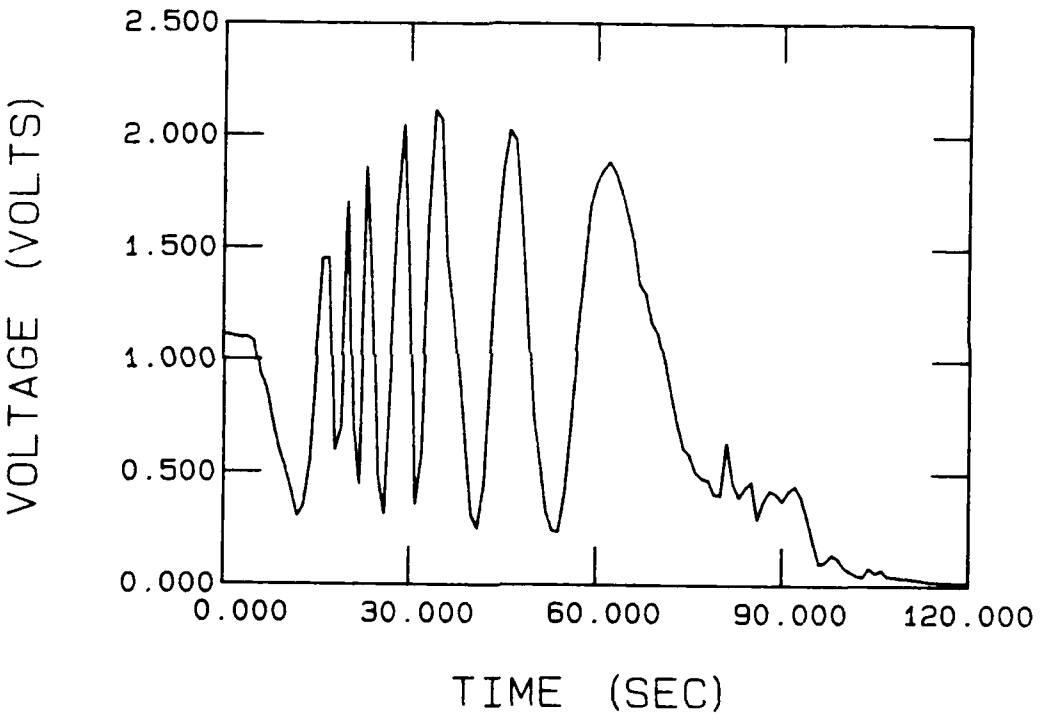

Figure 13. Fringe Readings

The sudden degrading of the fringe pattern was believed to be the point of rapid shear failure. The data from the LISG was plotted and the average fringe motion was converted to a relative displacement (see Figure 14).

Figure 14 shows the displacement between the fracture surfaces of the beam. Like our previous load displacement curve, there is initially a linear relationship between load and displacement. At a load of 225 pounds the relationship becomes nonlinear. At this point, the rate of displacement between indents increased greatly. This trend is consistent with the rapid shear failure of a brittle material.

The load of 225 pounds was only three pounds lower than the point of nonlinearity on the load-load point displacement curve. This backs up our theory on critical load . The point of nonlinearity from all the load-load point displacement curves was then used as the critical load in the calculation of G_{IIc}.

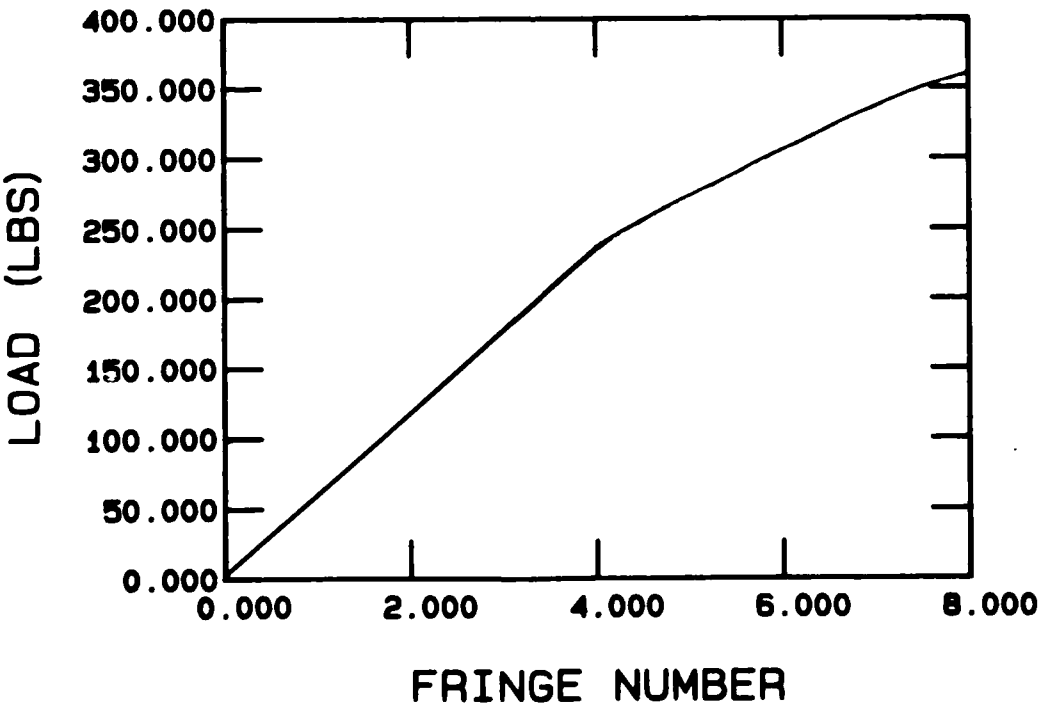

Figure 14. Relative Displacement of Shear Plane

Critical Energy Release Rate

The instant of crack initiation was taken at the point of nonlinearity as described earlier. The values of critical load, that were required for the calculation of the strain energy release rate, were now available. A chart of critical load vs. crack length was prepared (see Figure 15). Finally, an analytical and an experimental value of the strain energy release rate was calculated for each of the fractured specimens. The analytical energy release rate was based on the earlier theoretical compliance expression and the simple beam theory. The analytical equation used was (17):

$$G_{II} = \frac{9P^2a^2}{16b^2E_{11}h^3} \qquad (4)$$

where

P = load

a = initial crack length

b = specimen depth

E_{11} = Young's Modulus

h = specimen height

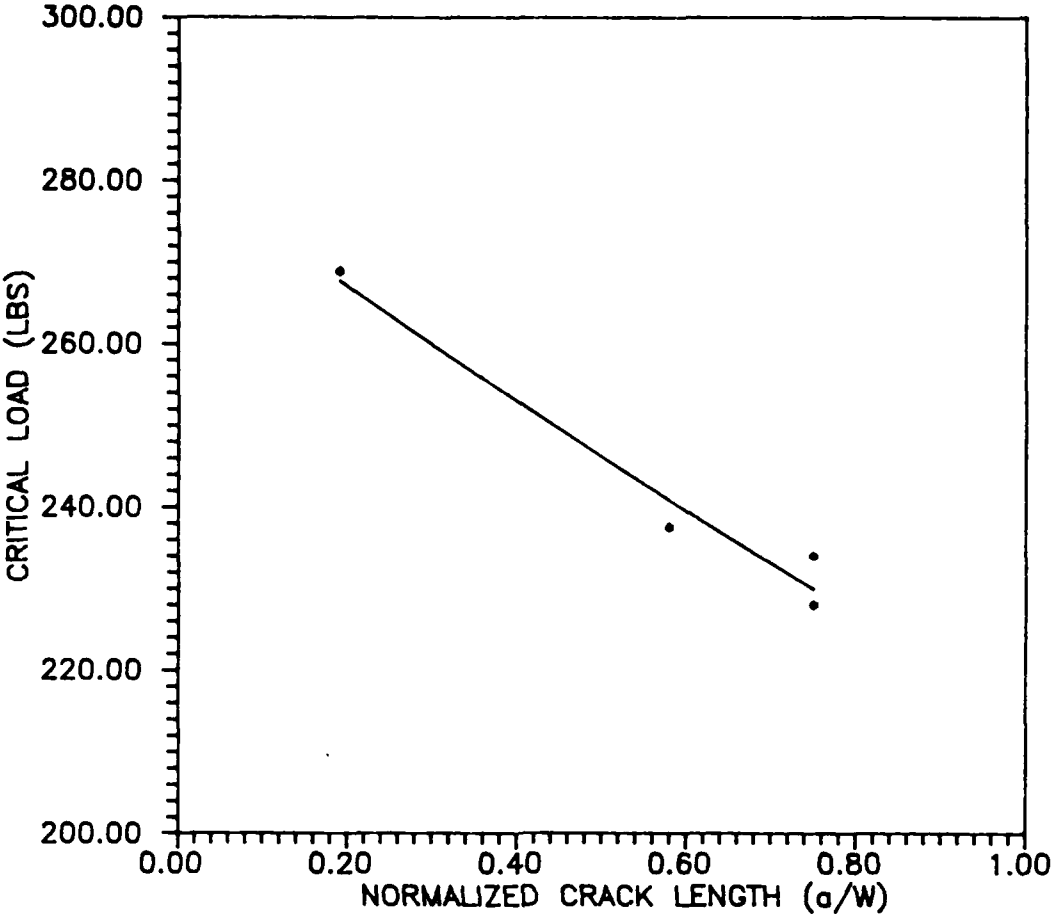

Figure 15. Critical Load vs. Crack Length

The critical strain energy release rate was calculated using the expression:

$$G_{IIc} = (P_c^2/2B)(dC/da) \qquad (5)$$

The value of dC/da was found from the derivative of the compliance curve that was plotted earlier (see Figure 11).

The critical strain energy release rate was calculated for each crack length and compared to the corresponding value obtained from the analytical value of G_{II} (see Table IV).

Table IV. Mode II Fracture Toughness

Crack Length (in)	Critical Load (lbs)	G Experimental (lb/in)	G Theoretical (lb/in)
.1405	268.8	2.165	4.860
.5625	228.1	2.114	7.410
.563	234.4	2.233	7.839

The experimental values of G_{IIc} were within five percent of each other. This was an expected result if the critical strain energy release rate was a material property. Since the values were so consistent, it gives an indication that the test was conducted properly and that the assumptions that were made were correct.

The analytical values of G_{II}, however, not only differed from the experimental results, but also differed greatly from each other. Both the theoretical expressions for compliance and strain energy release rate are based on simple beam theory. For small specimens and small crack lengths simple beam theory is not accurate. Other relationships have to be developed for the small specimen using finite element analysis or another analytical method.

Fracture Surface

After the fracture tests, the fracture surfaces were examined under a microscope at varying powers up to a maximum magnification of 200X. The specimens had already fractured up to the midspan loading point. To view those fracture surfaces, the remaining half of the neutral plane was separated using a Mode I type pulling force. This left a fracture surface that could be divided into four general sections: the notch, the pre-crack, the shear fracture, and the Mode I failure (See Figure 16).

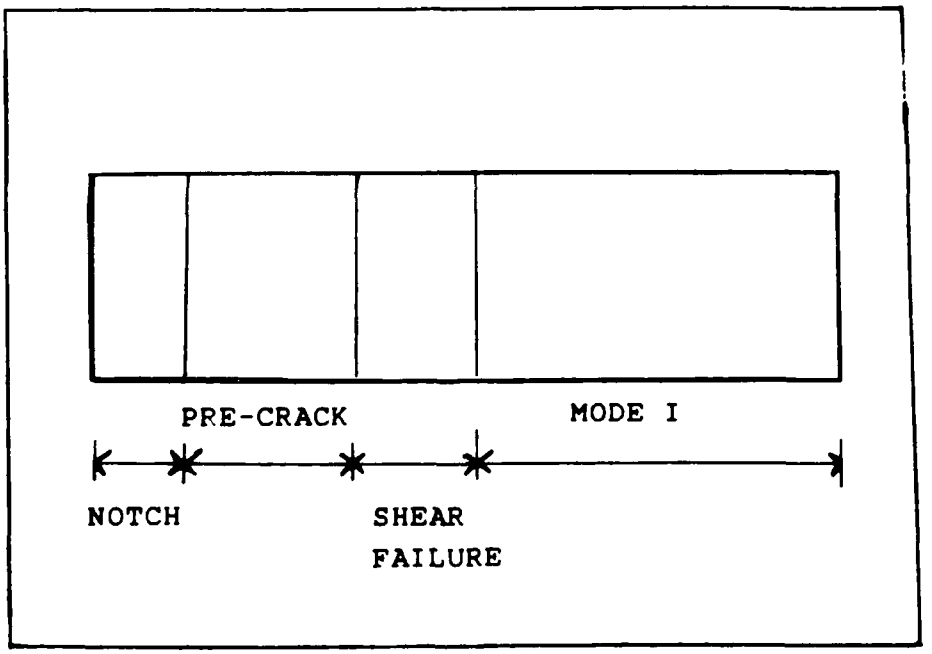

Figure 16. One Fracture Surface

(Top View)

The area of the notch was evident in the photographs (see Figure 17). It showed the effects of the diamond grinding that resulted from the use of the diamond wheel. The notch and the pre-crack show a dramatic change in surface. The pre-crack had a smooth planer surface that continued until it blends into the area of shear failure. There was very little difference between the pre-crack and Mode II fracture. The two ran in the same plane. The surfaces were smooth with relatively few instances of fiber pull out.

The similarity of the pre-crack and failure gave another indication of a good test, since the pre-crack gave the appearance of a natural fracture. The fracture plane was evidence of pure brittle fracture without ductility. The probable failure mechanism was in the fiber-matrix interface or in the matrix itself.

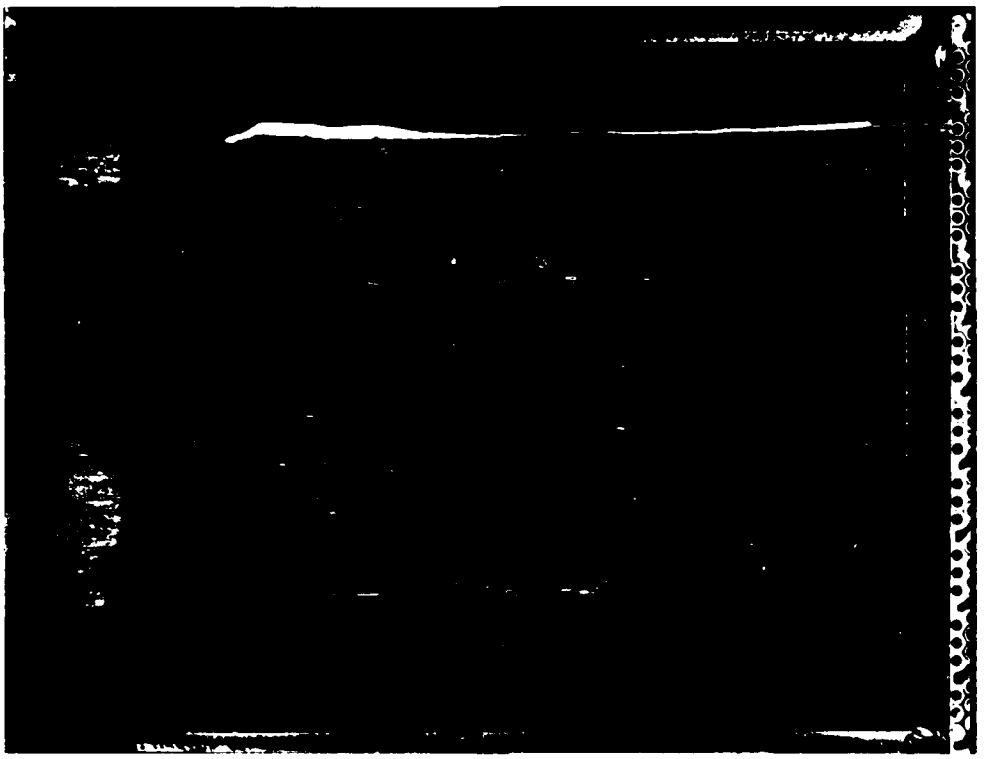

Figure 17. Fracture Surface - Mode II
Diamond ground notch (left), and
Mode II surface (right).

The area of Mode I failure was not as smooth as the first half of the specimen (See Figure 18). The Mode I surfaces exhibited much more destruction to the fibers than was evident in the Mode II failures.

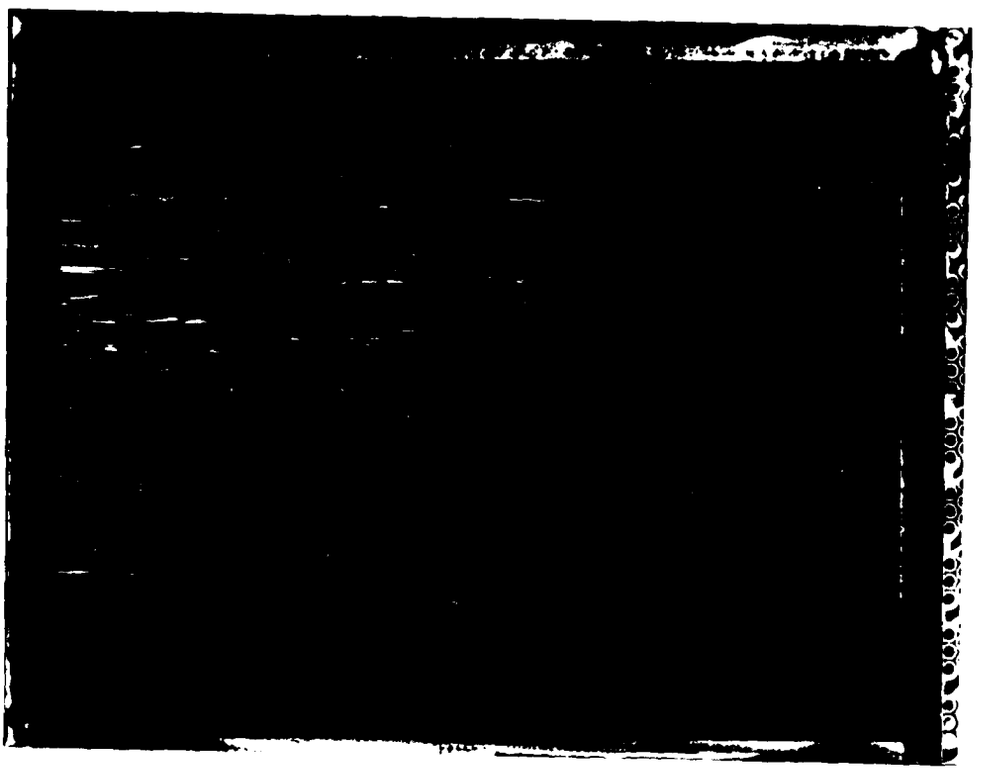

Figure 18. Fracture Surface - Mode I

Magnification 15X

CONCLUSIONS AND RECOMMENDATIONS

The initial objective of this study was to develop a technique that could be used for fracture toughness testing of small composite specimens. The technique was to be developed so that it could be modified for use at elevated temperatures. Finally, this technique was to test some ceramic matrix composite specimens. Based on the completed test, there are several conclusions to be made:

Conclusions

1) A test method for finding the critical strain energy release rate, G_{IIc}, for a small ceramic matrix composite specimen was developed.

2) The end-notched flexure specimen is a viable specimen for Mode II testing of small composite specimens.

3) The LISG provided the instant of crack initiation, which corresponded to the point of nonlinearity on the load-displacement curve.

4) G_{IIc} was found for the 1723 glass matrix, silicon carbide fiber composite.

5) The analytical expressions for compliance and strain energy release rate need to be modified for use with small composite specimens.

Recommendations

Based on this study, some recommendations of further study can be made.

1) Replace the manual loading device with a finely adjustable, automated loading device. An automated device such as an MTS would allow for much smoother loading rates, loading control and displacement control. It would also allow for cyclic loading, which is needed for fatigue testing. This would alleviate many of the short comings of our present experimental set-up.

2) Improve the existing computer program or write a new program that would allow for more rapid acquisition, more input variables, and varied output. For the rapid failures associated with brittle glasses, data needs to be acquired more than once a second to accurately measure the fracture growth. The present software can only collect data once a second. Also, our technique uses load point displacements versus loads to find specimen compliances. The present computer program was not designed with compliances in mind or G_{II} in mind.

3) Apply this technique to other modes of fracture. Other composite orientations could be used to investigate Mode I or Mixed Mode I and II.

4) One large area of further study would be to apply a variation of this technique to high temperature applications. The LISG and tabbing have been applied to

temperatures up to 1400°C. This work was applied to Mode I failure, however, and could now be expanded to include Mode II fracture. This would involve major changes in material and equipment.

APPENDIX A

The composite used in this study was manufactured at the Air Force Materials Laboratory, Wright Patterson AFB. Larry Zawada (ref. 37), an engineer in the Materials Laboratory provided the direction for the composite fabrication which was based on general concepts worked by Karl Prewo and others (ref. 7-9, 28-36).

Materials

The basic components of the composite are an aluminosilicate glass frit, a binder solution, and the silicon carbide yarn. The glass frit consisted of a 1723 Corning amorphous glass mixture which comes in the form of a finely ground powder. The R Hoplex Binder was in the form of a liquid. The silicon carbide fibers were in the form on a Nicalon yarn manufactured by the Nippon Carbon Company of Tokyo.

The composite was manufactured by the hot pressing of multiple layers of infiltrated unitape. The process of making the unitape begins with the mixing of a liquid slurry. The slurry is composed of a mixture of glass, binder and water. The specific combination used was:

80 grams 1723 Corning Glass Frit

210 milliliters Distilled Water

90 milliliters R Hoplex Binder

Winding

After the slurry has been well mixed, it was used to coat the silicon carbide yarn. The slurry-impregnated yarn was then wound on a mandrel to form unidirectional tapes (see Figure 19).

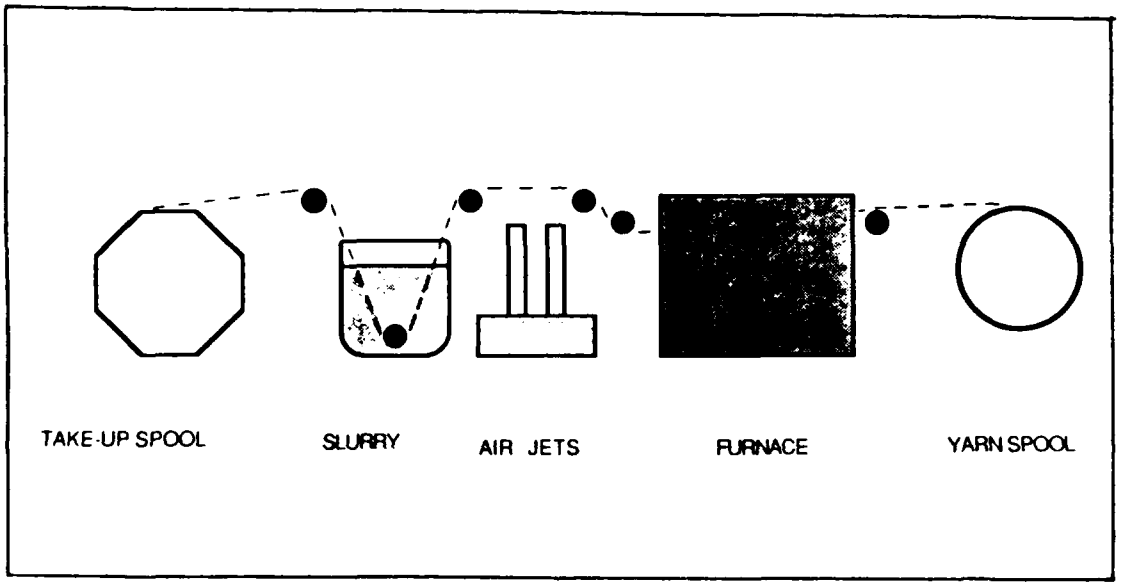

Figure 19. Winding Process

The winding process was performed manually and each four hour winding produced eight four inch wide plies. The winding was performed by mounting a spool of silicon carbide yarn on a roller at one end of a long work table. A single strand of silicon carbide yarn was gradually pulled through

a hot furnace set a 600 degrees centigrade. As the yarn was pulled through the furnace, a protective coating was burned from the yarn. This left only the silicon carbide material itself. The uncoated yarn was then directed over a set of air jets. The air jets teased the strands of yarn and loosened the bundles of fiber. The loosened yarn was then run through a beaker of the slurry. The slurry was kept constantly agitated by a magnetic spinner located at the bottom of the beaker. The agitation insured a constantly uniform mixture within the slurry and also insured a well impregnated yarn coming out of the slurry. The yarn was then carefully wound on a slowly rotating mandrel. The mandrel was in the form of an octagon with four inch by six inch faces. The slurry impregnated yarn was continuously wound on the mandrel until a four inch wide tape was formed. The tape was formed by multiple parallel windings of yarn with a half diameter overlap on each winding. As the winding progressed, the yarn was gently flattened to ensure that the individual strands of yarn became sufficiently meshed together. A heating lamp was used to slowly dry the newly formed tape on the rotating mandrel. The binder dried to form a rigid tape of fiber and matrix.

Once dry, the unidirectional tape was cut from the mandrel. Each of the eight faces on the mandrel provided a single rough ply approximately four inches by six inches in

size. These rough plies were then cut into smaller plies using a paper cutter. Depending on the final specimen size desired, each rough ply was then cut into four, two by two inch plies or one, four by four inch ply. Each finished ply was visually inspected to insure the quality of the tape. These ply sizes were determined by the molds used in the hot pressing. The specimen thickness was determined by the number of plies stacked together during hot pressing. It took forty plies to achieve our 0.2 inch thick specimen.

Hot Pressing

To make our final unidirectional sample forty plies were stacked in a special graphite die. The inside of the die was lined with tantalum foil to prevent sticking. Molybdenum foil was placed on top of and below the forty plies also to prevent sticking. Finally, graphite plungers were placed in the die and the layers were compacted in a vice.

The graphite die was then placed in a hot press and a thermocouple was inserted into the upper plunges. The hot press was gradually heated to 800 degrees centigrade and the pressure was increased to 500 pounds per square inch. During this time the binder was burned off and any excess gases escaped from the die. The composite was then rapidly heated to a temperature of 1100 degrees centigrade and the pressure

was increased to 1800 pounds per square inch; the composite was held at this final state for ten minutes and then gradually cooled.

The whole process took five hours with constant monitoring by an engineer. The hot press temperature, pressure, and ram displacement were recorded every ten minutes during the run. The engineer looked for trends in the relationships between displacement and temperature based on previous hot pressings of this ceramic composite. This provided one measure of quality control during the fabrication process.

The result of the process was a four by four inch square that was 0.2 inches thick. Surface quality was good and fiber distribution was good (see Figure 20) with about 50 percent volume of fiber. The photograph shown in Figure 19 was taken of a cross section at the center of the four by four inch composite plate. The volume of fiber was calculated from the fiber surface visible in a photomicrograph of the composite.

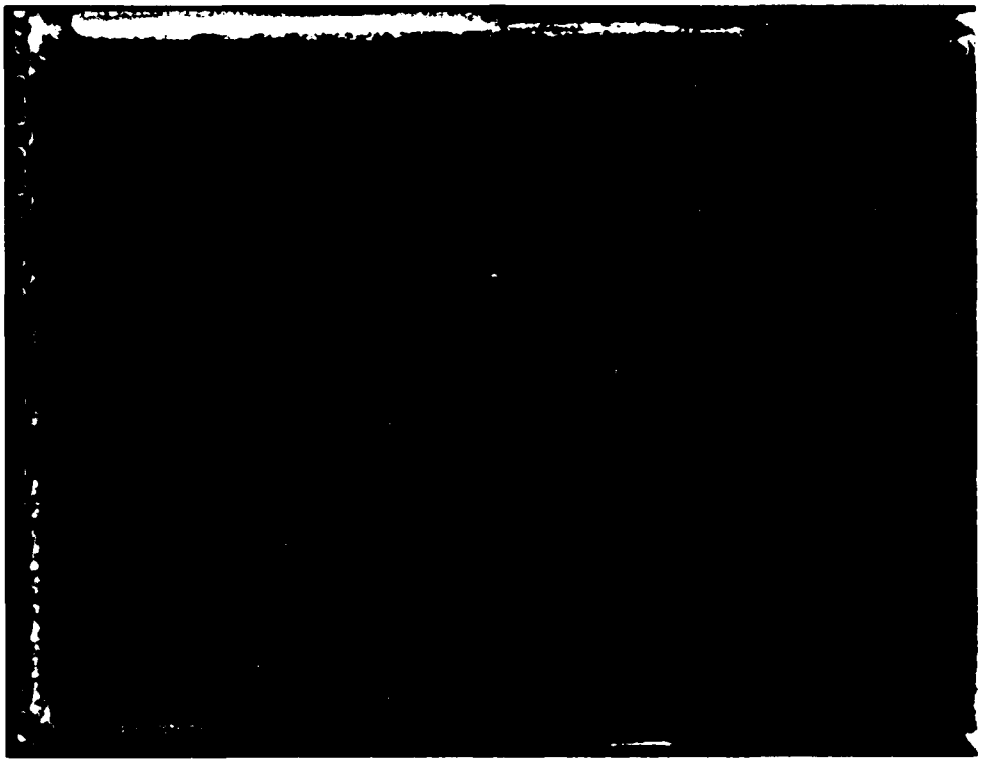

Figure 20. Microstructure of 1723 Glass Composite

Magnified X100

Appendix B

After the compliance measurements were taken, five specimens were loaded until fracture. The load vs. load point displacement curves are included in the following pages (see Figures 20-24). It was difficult to visually determine the exact point of shear failure; therefore, the load-displacement curves were used to determine the critical load at which the shear fracture propagated.

Each curve exhibits similar trends. Initially, the load-displacement relationship was linear. At a certain point the curves deviated from the initial course and became nonlinear. Finally, the load dropped off.

The point of nonlinearity determined the critical load. It can be seen that the load at the point of nonlinearity decreases with increasing crack length.

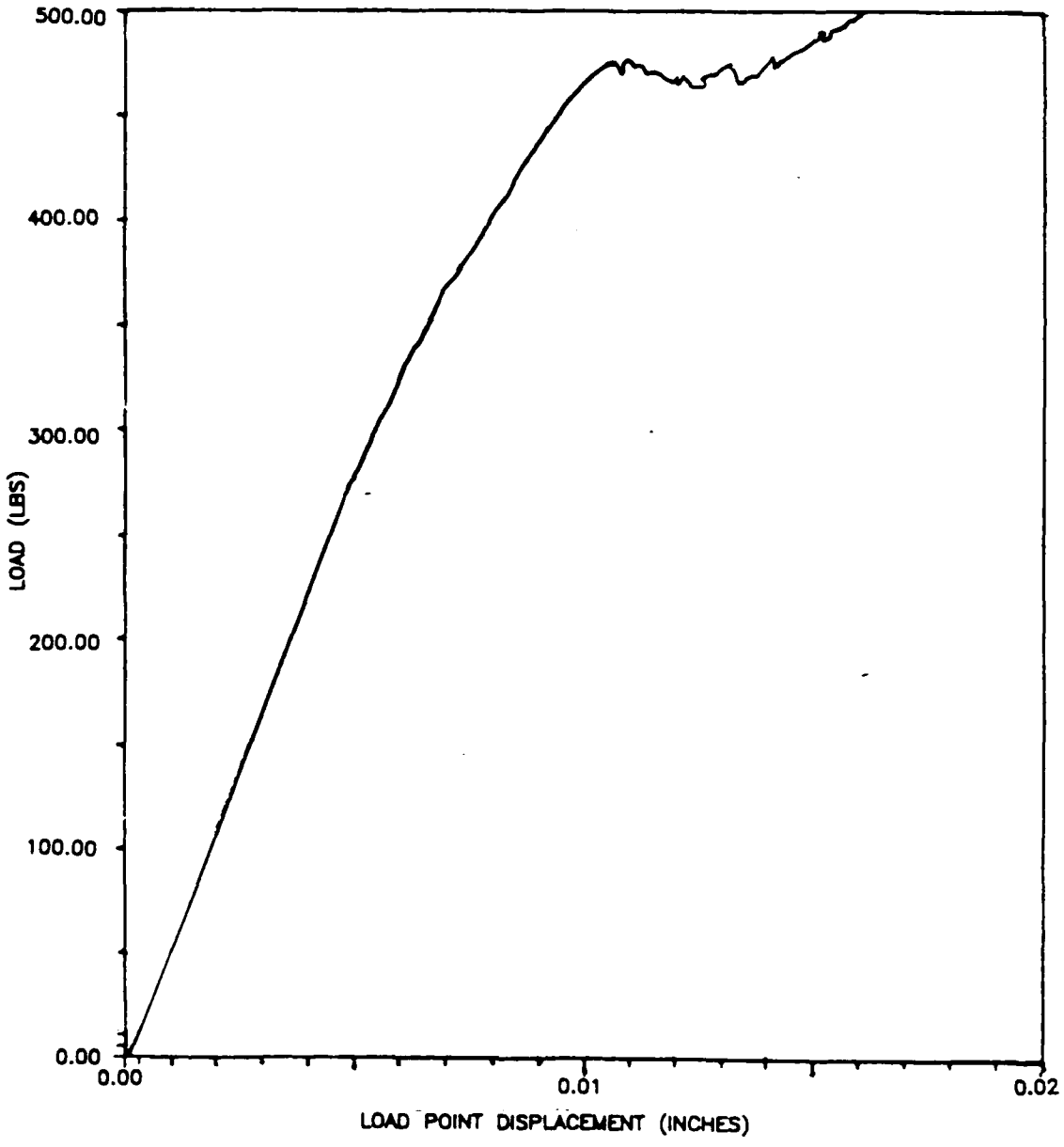

Figure 21. Experimental Plot, a/W = .187

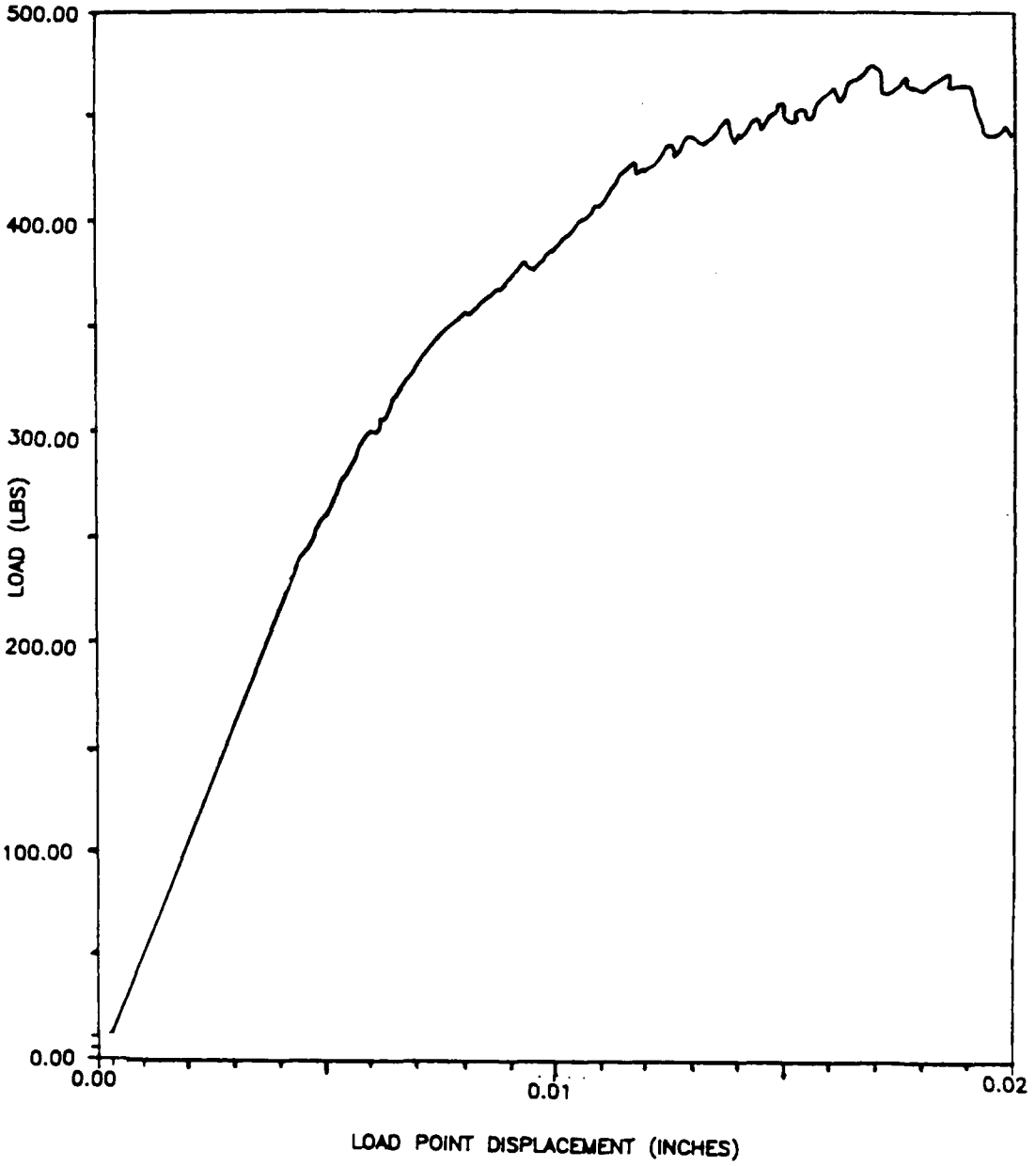

Figure 22. Experimental Plot, a/W = .583

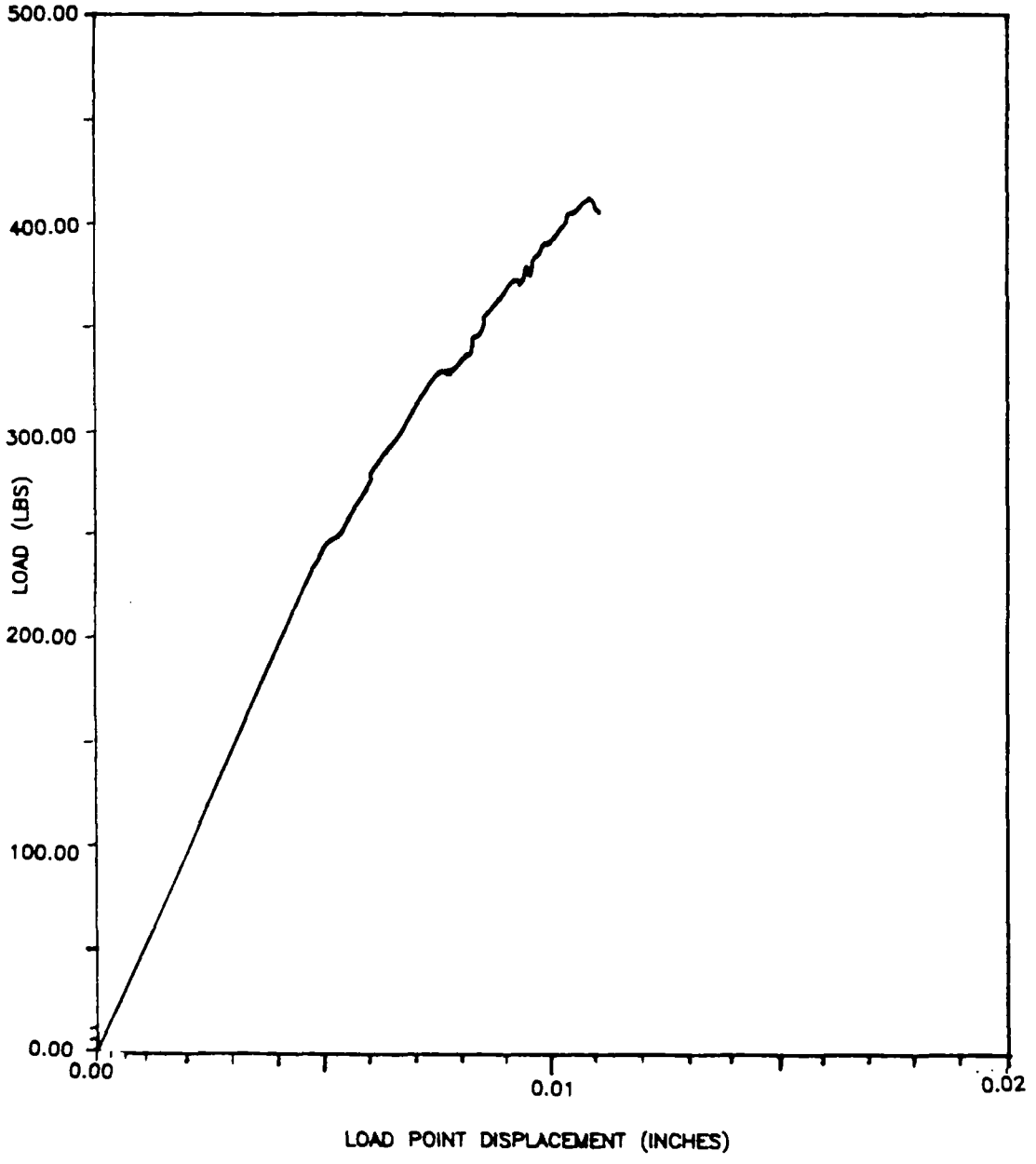

Figure 23. Experimental Plot, a/W = .750

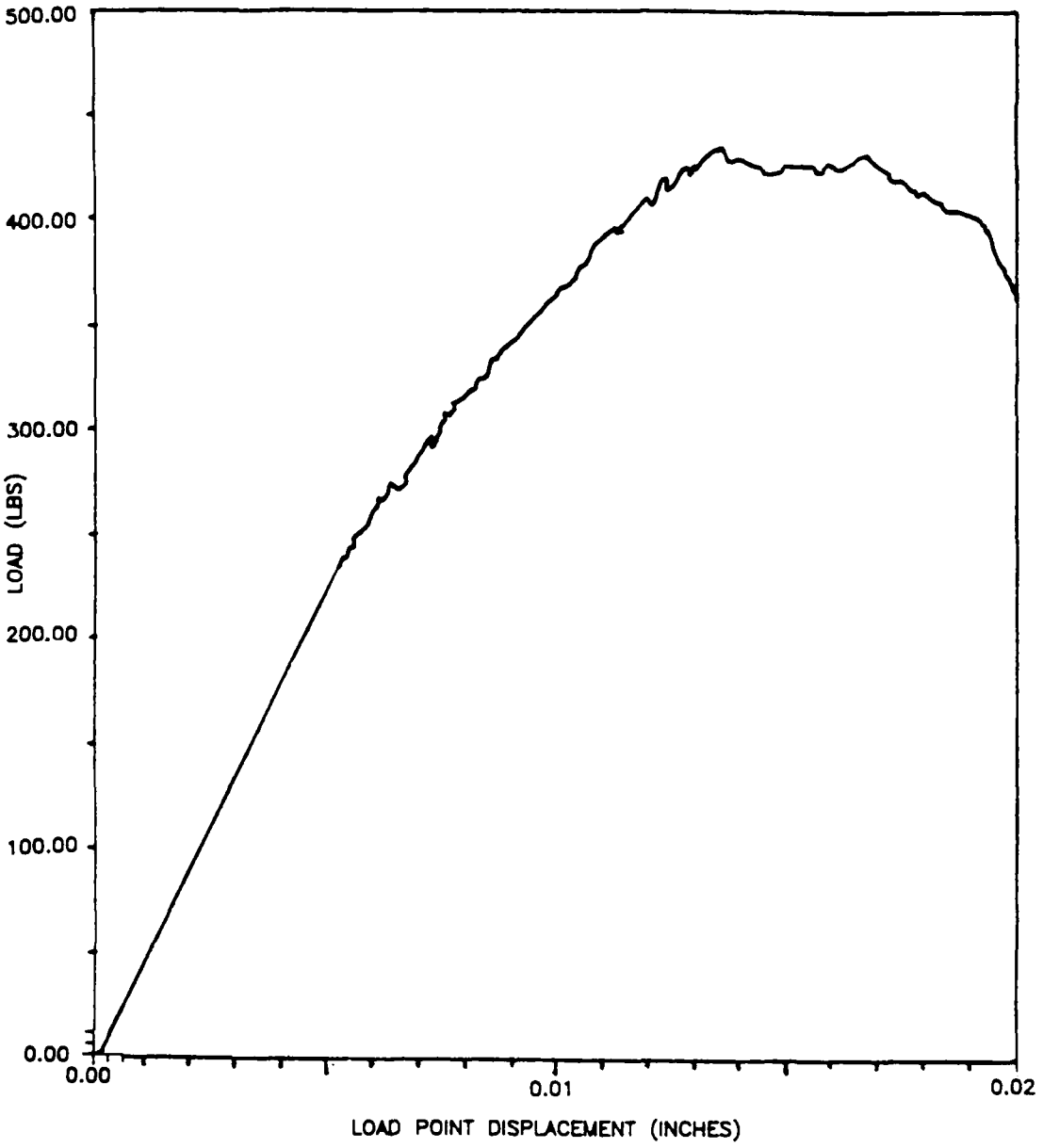

Figure 24. Experimental Plot, a/W = .751

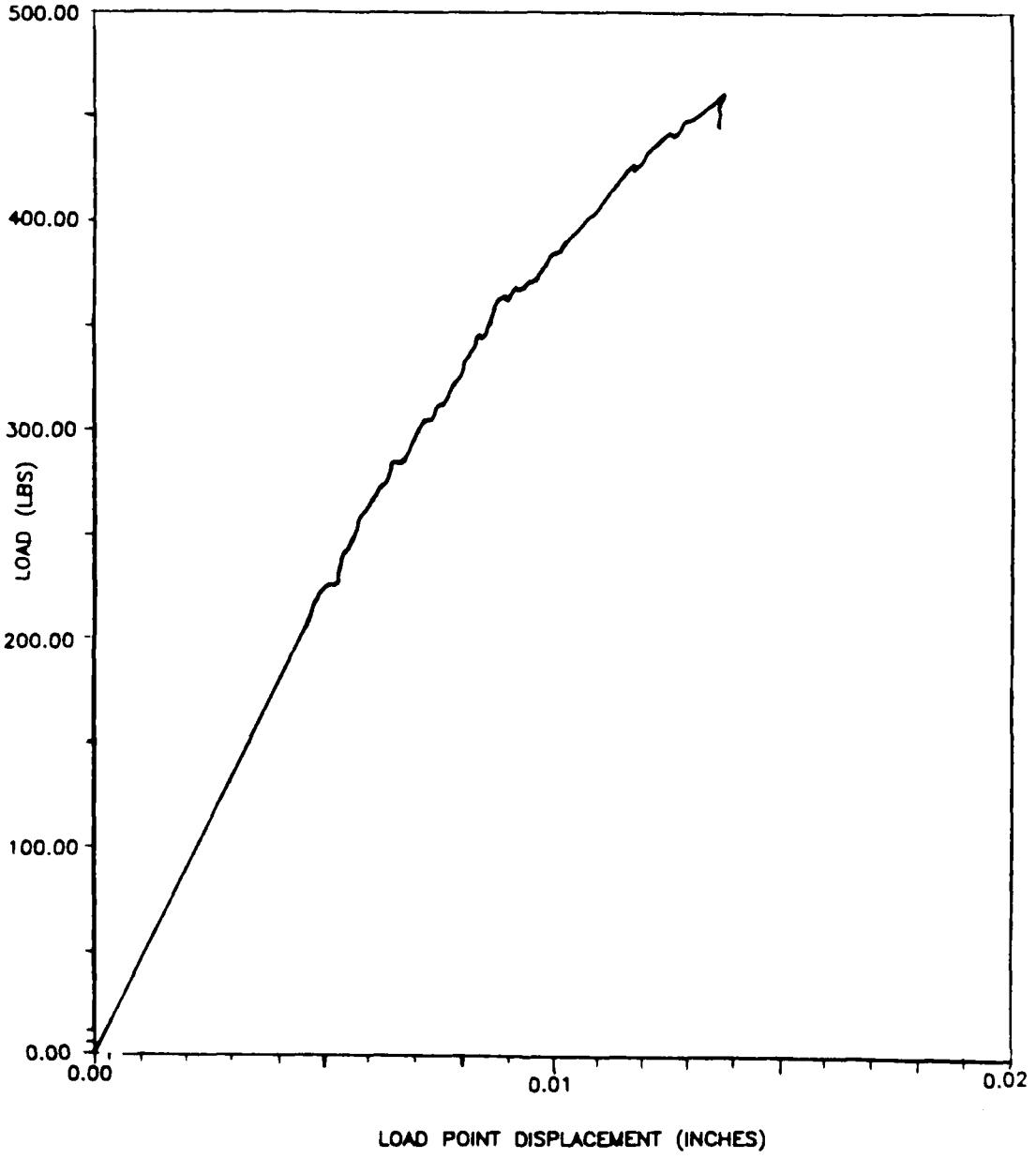

Figure 25. Experimental Plot, a/W = 1.000

Appendix C

Computer Program

The following computer program was written by Jay Jira of the Air Force Materials Laboratory (AFWAL/MLLN), for use with a laser interferometric strain gauge. The program was run on a Tektronix 4052 computer with an auxiliary memory. The program recorded the output voltages from the two photo-multiplier tubes and the load cell. The program allows the user to input information about the specific operating parameters of the equipment and the desired data reading rate. The input voltages were then converted to the appropriate units and were recorded in memory. The computer program processed the load and fringe information into the form of relative displacements. It was then possible to select various plots of load, displacement and time.

```
4 PRINT "LDO YOU WANT TO INITIALIZE? (Y/N) ";
5 INPUT Z$
6 IF Z$="Y" THEN 100
20 GO TO 130
24 Z=1
25 PRINT "G";
26 RETURN
32 PRINT P;"H";
33 RETURN
36 Z=2
37 PRINT "G";
39 RETURN
40 Z=3
42 PRINT "G";
43 RETURN
100 INIT
110 A9=0
120 GO TO 570
130 REM ********************* THIS SECTION GIVES MENU ******************
140 PRINT @32,26:0
150 PRINT "LGI        LASER INTERFEROMETRY"
160 PRINT "IHHHHH   DATA AQUISITION   DISPLACEMENT/TIME/LOAD"
170 PRINT "I              VERSION #5"
180 REM ******************** JAY R. JIRA ***************************
190 REM ******************** DECEMBER 1983 *************************
200 PRINT "JJI          ***** MENU *****"
210 PRINT "IJINITIALIZE PARAMETERS ---------- (1)"
220 PRINT "ILIST/CHANGE PARAMETERS ---------- (2)"
230 PRINT "ITAKE NEW DATA ------------------- (3)"
240 PRINT "IPROCESS DATA -------------------- (4)"
250 PRINT "ILIST UNPROCESSED DATA ----------- (5)"
260 PRINT "ILIST PROCESSED DATA ------------- (6)"
270 PRINT "IPLOT UNPROCESSED DATA ----------- (7)"
280 PRINT "IPLOT PROCESSED DATA ------------- (8)"
```

```
290 PRINT "ITRANSFER DATA FILE TO PDP ------- (9)"
300 PRINT "ICALCULATE LOAD FOR A GIVEN K ---- (10)"
310 PRINT "ISET CLOCK ---------------------- (11)"
320 PRINT "ITERMINAL MODE ------------------ (12)"
330 PRINT "IPRINT TIME --------------------- (13)"
340 PRINT "IMEMORY CHECK ------------------- (14)"
350 PRINT "IAUTO UPDATE -------------------- (15)"
360 PRINT "IJCHOOSE ONE: ";
370 INPUT Z$
380 IF Z$="" THEN 130
390 Z=VAL(Z$)
400 IF A9=0 AND (Z=2 OR Z=3) THEN 440
410 GO TO Z OF 700,1470,1550,2700,4810,5280,5660,6160,7350,7950,610,7860
420 GO TO Z-12 OF 670,520,460
430 GO TO 130
440 PRINT "YOU MUST INITIALIZE PARAMETERS FOR THIS OPERATION"
450 GO TO 360
460 PRINT "JINSERT TAPE - RETURN ";
470 INPUT Z$
480 FIND 2
490 SAVE
500 CALL "MSAVE",100
510 CALL "MLINK",101,90
520 REM ***** MEMORY CHECK ROUTINE *****
530 CALL "MSPACE",Z
540 PRINT "JAUXILLIARY MEMORY AVAILABLE:   ";Z;" BYTES"
550 PRINT "J       4051 MEMORY AVAILABLE:   ";MEMORY;" BYTES"
560 GO TO 360
570 REM ***** THIS SECTION SETS CLOCK *****
580 PRINT "JDO YOU NEED TO RESET CLOCK? (Y/N) ";
590 INPUT Z$
600 IF Z$="N" THEN 660
610 PRINT "JINPUT DATE/TIME IN THIS FORMAT: 24-AUG-83 13:30:05 ";
620 DELETE Z$
630 DIM Z$(18)
```

```
640 INPUT Z$
650 CALL "SETTIM",Z$
660 GO TO 130
670 CALL "TIME",Z$
680 PRINT "JTHE TIME IS: ";Z$
690 GO TO 360
700 REM ********** THIS SECTION INITIALIZES PARAMETERS **************
710 FOR I=1 TO 8
720 GOSUB I OF 760,830,950,1110,1150,1250,1310
730 NEXT I
740 A9=1
750 GO TO 130
760 REM **** INITIALIZE TEST I.D. ****
770 PRINT "JINPUT SPECIMEN/TEST I.D.(40 CHAR MAX) "
780 PRINT "JEXAMPLE: MATERIAL/LASER INT./SPEC.NUMBER/K VALUE/LENGTH "
790 PRINT "JI.D.="
800 PRINT "     ----------------------------------------KK_     ";
810 INPUT A$
811 IF A$<>"" THEN 820
812 A$="NO I.D."
820 RETURN
830 REM **** INITIALIZE BITS ****
840 PRINT "JINPUT 8 OR 12 BIT RESOLUTION (8,12,OR I=INSTRUCTIONS) ";
850 INPUT Z$
860 IF Z$<>"I" THEN 890
870 GOSUB 3750
880 GO TO 840
890 V$="8BIT"
900 B=1
910 IF Z$="8" THEN 940
920 V$="12BIT"
930 B=2
940 RETURN
950 REM **** INITIALIZE GAIN (CHANNEL SEQUENCE) ****
960 DIM R(2),C(2)
```

```
970 C(1)=1
980 C(2)=2
990 PRINT "LUSE CHANNELS 1 AND 2 ON TRANSERA FOR PMT INPUTS"
1000 PRINT "JINPUT GAIN DESIRED ON TRANSERA INPUT CHANNELS:"
1010 PRINT "IPHOTOMULTIPLIER #1 (1,4,32,0=INSTRUCTIONS) ";
1020 INPUT R(1)
1030 IF R(1)=0 THEN 1070
1040 PRINT "IPHOTOMULTIPLIER #2 (1,4,32,0=INSTRUCTIONS) ";
1050 INPUT R(2)
1060 IF R(2)<>0 THEN 1090
1070 GOSUB 3750
1080 GO TO 1000
1090 PRINT "GJ       CHAN. #3 RESERVED FOR LOAD SIGNAL (0-10 VOLT MAX)"
1100 RETURN
1110 REM ***** INITIALIZE LOAD CALIBRATION *****
1120 PRINT "JINPUT LOAD CALIBRATION FACTOR (LBS/VOLT) ";
1130 INPUT G
1140 RETURN
1150 REM ***** INITIALIZE LENGTH OF TEST *****
1160 PRINT "JINPUT LENGTH OF TEST (MINUTES) (0=CALCULATE FROM HOURS) ";
1170 INPUT L
1180 IF L=0 THEN 1210
1190 IF L>0 THEN 1240
1200 GO TO 1160
1210 PRINT "IJINPUT LENGTH OF TEST IN HOURS ";
1220 INPUT L
1230 L=L*60
1240 RETURN
1250 REM **** INITIALIZE PERIOD ****
1260 PRINT "JINPUT DESIRED PERIOD BETWEEN SCANS - SECONDS (P>=1) ";
1270 INPUT P
1280 IF P<=0 THEN 1260
1290 REM ***** SUBROUTINE PROTECTS AGAINST INSUFFICIENT DATA SPACE ****
1300 RETURN
1310 REM **** INITIALIZE HEADER (AND DATA) FILE AND SIZE ****
```

```
1320 PRINT "JINFORMATION CONCERNING THIS TEST WILL BE STORED ON A"
1330 PRINT "HEADER FILE .  RAW DATA WILL THEN BE STORED ON THE NEXT"
1340 PRINT "IMMEDIATE FILE.  (2 FILES UTILIZED PER TEST) "
1350 PRINT "JINPUT HEADER FILE NUMBER (AUTO MARKED 200 BYTES) ";
1360 INPUT F1
1370 RETURN
1380 REM ***** SUBROUTINE PROTECTS AGAINST INSUFFICIENT DATA SPACE ****
1390 IF L*60/P*40<290000 THEN 1460
1400 PRINT "JGGGGG  ERROR !!!     INSUFFICIENT TAPE SPACE FOR THE LENGTH"
1410 PRINT "AND PERIOD SPECIFIED - EVEN WITH A NEW 300K DATA TAPE"
1420 PRINT "DECREASE LENGTH OR INCREASE PERIOD OR DATA MAY BE LOST."
1430 PRINT "JPRESS RETURN TO CHANGE PARAMETERS ";
1440 INPUT Z$
1450 GO TO 130
1460 GO TO 1590
1470 REM ********** THIS SECTION MAKES A PARAMETER CHANGE **********
1480 PAGE
1490 GOSUB 3580
1500 PRINT "JJINPUT LINE NUMBER OF CHANGE (0=NO CHANGE) ";
1510 INPUT Z
1520 IF Z=0 THEN 130
1530 GOSUB Z OF 760,830,950,1110,1150,1250,1310
1540 GO TO 1480
1550 REM ****** DATA AQUISITION, PROCESSING AND STORAGE ON TAPE ******
1560 PRINT "LJINSERT TAPE FOR DATA STORAGE: PRESS RETURN ";
1570 INPUT Z$
1580 GO TO 1380
1590 PRINT "JPRESS RETURN TO START DATA AQUISITION "
1600 PRINT "JJWARNING: WAIT FOR AXIS TO BE DRAWN !!!G"
1610 FIND F1
1620 MARK 1,200
1630 FIND F1
1640 CALL "TIME",T$
1650 WRITE @33:N$,"TENSILE",T$,"RUNNING",U$,L,P,F1,R(1),R(2),L*60/P,0,G
1660 CLOSE
```

```
1670 DELETE A$,B$,A1,B1,C1,C2
1680 REM ***** N0=NO. OF PNTS. AVERAGED INTO EACH PMT SCAN
1690 REM ***** R0= TIME INCREMENT(SECS) BETWEEN EACH PNT.
1700 N0=10
1710 R0=0.025
1720 DIM A$(B*N0),B$(B*N0),A1(N0),B1(N0),C1(3),C2(3)
1730 SET KEY
1740 CALL "OPEN",1,1,8
1750 A$=""
1760 B$=""
1770 A1=0
1780 B1=0
1790 U=0
1800 N1=0
1810 T1=0
1820 C1=0
1830 C2=0
1840 C4=0
1850 H=0
1860 Z=0
1870 S0=2↑(3+4*B)
1880 FIND F1
1890 GOSUB 3890
1900 GOSUB 4240
1910 PRINT "GGGGGGGGGGGGGGGG"
1920 INPUT Z$
1930 N1=N1+1
1940 IF P=1 THEN 2100
1950 CALL V$
1960 CALL "BURST",A$,N0,R0,1,0,R(1)
1970 CALL "128IT"
1980 CALL "TIME",T$
1990 CALL "A/D",C4,3
2000 CALL V$
2010 CALL "BURST",B$,N0,R0,2,0,R(2)
```

```
2020 GOSUB 3960
2030 T2=T
2040 CALL "UNPAK2",A$,A1,N0,B,S0,S0*0.1
2050 CALL "UNPAK2",B$,B1,N0,B,S0,S0*0.1
2060 C2(1)=SUM(A1)/N0
2070 C2(2)=SUM(B1)/N0
2080 C2(3)=C4
2090 GO TO 2160
2100 REM ***** DATA ACQU. SEQ. FOR 1 SEC PERIOD *****
2110 CALL "12BIT"
2120 CALL "A/D",C2
2130 CALL "TIME",T$
2140 GOSUB 3960
2150 T2=T
2160 CALL "WRITE",1,T2,C2(1),C2(2),C2(3)*G
2170 IF N1=1 THEN 2260
2180 VIEWPORT 3,130,51,92
2190 MOVE T1,C1(1)
2200 DRAW T2,C2(1)
2210 VIEWPORT 3,130,4,45
2220 MOVE T1,C1(2)
2230 DRAW T2,C2(2)
2240 MOVE T1,C1(3)
2250 DRAW T2,C2(3)
2260 C1=C2
2270 T1=T2
2280 IF T2=>L*60 OR Z=1 THEN 2470
2290 GO TO Z OF 2470,2310,2360
2300 GO TO 2390
2310 IF P=1 THEN 2390
2320 P=P-1
2330 PRINT P;"H";
2340 Z=0
2350 GO TO 2390
2360 P=P+1
```

```
2370 PRINT P;"H";
2380 Z=0
2390 CALL "TIME",T$
2400 GOSUB 3960
2410 T3=T
2420 CALL "TIME",T$
2430 GOSUB 3960
2440 IF T=T3 THEN 2420
2450 IF T=>T2+P THEN 1930
2460 GO TO 2390
2470 COPY
2480 PRINT "LJGGGGGGDATA AQUISITION COMPLETE","TIME= ";T$
2490 PRINT "J              ";N1;" SCANS MADE   ";N1*3;" DATA VALUES TAKEN"
2500 REM ***** THIS SECTION STORES ACTUAL VOLTAGE DATA ON TAPE *****
2510 FIND F1
2520 WRITE @33:N$,"TENSILE",M$,T$,U$,L,P,F1,R(1),R(2),N1,0,G
2530 CLOSE
2540 FIND F1+1
2550 MARK 1,N1*40
2560 FIND F1+1
2570 DIM B3(4)
2580 CALL "SETIP",1,1
2590 FOR I=1 TO N1
2600 CALL "READ",1,B3
2610 WRITE @33:B3
2620 NEXT I
2630 CLOSE
2640 PRINT "JRAW DATA STORED ON MAGNETIC TAPE - FILE ";F1+1
2650 PRINT "JJJPRESS RETURN FOR MENU ";
2660 INPUT Z$
2670 SET NOKEY
2680 CALL "KILL",1
2690 GO TO 130
2700 REM ********** DATA PROCESSING **********
2710 PRINT "JINSERT TAPE CONTAINING DATA TO BE PROCESSED "
```

```
2720 PRINT "JINPUT HEADER FILE NUMBER OF DATA: ";
2730 INPUT X3
2740 FIND X3
2750 GOSUB 3890
2760 FIND X3+1
2770 CALL "OPEN",1,1,8
2780 DELETE B3
2790 DIM B3(4)
2800 FOR I=1 TO X6
2810 READ @33:B3
2820 CALL "WRITE",1,B3
2830 NEXT I
2840 PRINT "JGGGINSERT TAPE FOR PROCESSED DATA STORAGE...PRESS RETURN"
2850 PRINT "JINPUT HEADER FILE NUMBER FOR PROCESSED DATA ";
2860 INPUT X3
2870 FIND X3
2880 MARK 1,200
2890 FIND X3+1
2900 PRINT "JJJMAX/MIN - POLYFIT ROUTINES NOW BEING EXECUTED"
2910 PRINT "GJWARNING: LEAVE DATA TAPE IN UNTIL TOLD OTHERWISE "
2920 DELETE A,A1,A2,A3,S,S2,X,Y,T3
2930 CALL "OPEN",2,1,8
2940 CALL "OPEN",3,1,8
2950 DIM A(2,4),A1(9,4),A2(3,4),A3(2,4),S(3),S2(3),X(9),Y(9),T3(5)
2960 REM ***** INITIALIZE DIRECTION OF VOLTAGE CHANGE *****
2970 S2=0
2980 CALL "SETIP",1,1
2990 CALL "READ",1,A
3000 FOR J=2 TO 3
3010 IF A(2,J)-A(1,J)>0 THEN 3040
3020 S(J)=-1
3030 GO TO 3050
3040 S(J)=1
3050 NEXT J
3060 REM ***** FIND PEAKS AND VALLEYS AND SAVE TIME AT THESE POINTS **
```

```
3070 FOR I=2 TO X6-1
3080 CALL "SETIP",1.I*4-3
3090 CALL "READ",1.A
3100 FOR J=2 TO 3
3110 IF (A(2,J)-A(1,J))*S(J)=>0 THEN 3250
3120 GOSUB 4360
3130 IF ABS(A(1,1)-Z7)>2*X2 THEN 3240
3140 IF S2(J)=0 THEN 3190
3150 IF ABS(A(1,1)-A3(J-1,1))>2*X2 THEN 3180
3160 IF ABS(A(1,1)-Z7)>ABS(A3(J-1,1)-A3(J-1,2)) THEN 3240
3170 GO TO 3200
3180 CALL "WRITE",J,A3(J-1,1),A3(J-1,2),A3(J-1,3),A3(J-1,4)
3190 S2(J)=S2(J)+1
3200 A3(J-1,1)=A(1,1)
3210 A3(J-1,2)=Z7
3220 A3(J-1,3)=A(1,4)
3230 A3(J-1,4)=Z6
3240 S(J)=S(J)*-1
3250 NEXT J
3260 NEXT I
3270 FOR J=2 TO 3
3280 CALL "WRITE",J,A3(J-1,1),A3(J-1,2),A3(J-1,3),A3(J-1,4)
3290 NEXT J
3300 REM ***** THIS SECTION WRITES FRINGE DATA TO TAPE *****
3310 S=0
3320 CALL "SETIP",2,1
3330 CALL "SETIP",3,1
3340 S2(1)=S2(2) MAX S2(3)
3350 FIND X3+1
3360 MARK 1,S2(1)*80
3370 FIND X3+1
3380 A=0
3390 FOR I=1 TO S2(1)
3400 FOR J=1 TO 2
3410 IF I>S2(J+1) THEN 3430
```

```
3420 CALL "READ",J+1,A(J,1),A(J,2),A(J,3),A(J,4)
3430 NEXT J
3440 WRITE @33:A(1,1),A(1,3),A(1,2),A(1,4),A(2,1),A(2,3),A(2,2),A(2,4)
3450 NEXT I
3460 CLOSE
3470 FIND X3
3480 WRITE @33:C$,D$,E$,F$,G$,X1,X2,X3,X4,X5,X6,S2(1)/2,X8
3490 CLOSE
3500 PRINT "␣FINISHED - PROCESSED DATA STORED ON TAPE - FILE ";X3+1
3510 PRINT "␣␣␣PRESS RETURN FOR MENU";
3520 INPUT Z$
3530 CALL "KILL",1
3540 CALL "KILL",2
3550 CALL "KILL",3
3560 DELETE A,A1,A2,A3,S,S2,X,Y,T3
3570 GO TO 130
3580 REM ***** THIS SUBROUTINE PRINTS PARAMETER LIST *****
3590 PRINT "I␣     CURRENT PARAMETER LIST"
3600 PRINT "␣␣I(1) I.D.= ";N$
3610 PRINT "I(2) RESOLUTION              = ";U$
3620 PRINT "I(3) PHOTOMULTIPLIER #1"
3630 PRINT "I              INPUT CHANNEL = ";C(1)
3640 PRINT "I              GAIN          = ";R(1)
3650 PRINT "I    PHOTOMULTIPLIER #2"
3660 PRINT "I              INPUT CHANNEL = ";C(2)
3670 PRINT "I              GAIN          = ";R(2)
3680 PRINT "I(4) LOAD CALIBRATION        = ";G;" LBS/VOLT"
3690 PRINT "I(5) LENGTH OF TEST          = ";L;" MIN."
3700 PRINT "I(6) PERIOD                  = ";P;" SECS"
3710 PRINT "I(7) HEADER FILE NUMBER      = ";F1
3720 PRINT "I    RAW DATA FILE NUMBER    = ";F1+1
3730 PRINT
3740 RETURN
3750 REM ** THIS SUBROUTINE PRINTS GAIN CHARACTERISTICS OF TRANSERA **
3760 PAGE
```

```
3770 PRINT "J                    RESOLVING POWER ,NOISE SIGNIFICANCE, AND "
3780 PRINT "                    VOLTAGE RANGE OF THE TRANSERA SYSTEM ARE"
3790 PRINT "                    PARTIALLY DEPENDENT UPON:"
3800 PRINT "IJ1) NUMBER OF BITS UTILIZED (8 OR 12)"
3810 PRINT "I2) GAIN (1,4 OR 32)"
3820 PRINT "JI              TABLE OF GAINS"
3830 PRINT "J            R","VOLTAGE","12 BIT","8 BIT"
3840 PRINT "           (GAIN)","RANGE","RESOLUTION","RESOLUTION"
3850 PRINT "J            1","+-10 VOLTS","5 mV","78 mV"
3860 PRINT "J            4","+-2.5 VOLTS","1.25 mV","20 mV"
3870 PRINT "J           32","+-0.3 VOLTS","0.25 mV","2.5 mV"
3880 RETURN
3890 REM ***** THIS SUBROUTINE PRINTS HEADER (TEST PARAMETERS AND ID) **
3900 READ @33:C$,D$,E$,F$,G$,X1,X2,X3,X4,X5,X6,X7,X8
3910 PRINT "L";C$;"  LENGTH:";X1;" (MIN)  LOAD CAL:";X8
3920 PRINT "#SCANS:";X6;"   PERIOD:";X2;"   HEADER FILE#:";X3;"   ";
3930 PRINT X7;"  FRINGES"
3940 PRINT "GAIN:";X4;"/";X5;"   ";G$;"   START:";E$;"   STOP:";F$
3950 RETURN
3960 REM *****  THIS SUBROU FINDS NUMBER OF SECONDS SINCE THE  ******
3970 REM ******************** TEST WAS STARTED ****************************
3980 T=0
3990 IF H=1 THEN 4010
4000 H$=SEG(T$,4,3)
4010 Z$=SEG(T$,4,3)
4020 IF Z$=H$ THEN 4100
4030 IF H$="FEB" THEN 4090
4040 IF H$="APR" OR H$="JUN" OR H$="SEP" OR H$="NOV" THEN 4070
4050 T=31*86400
4060 GO TO 4100
4070 T=30*86400
4080 GO TO 4100
4090 T=28*86400
4100 Z$=SEG(T$,1,2)
4110 T=T+VAL(Z$)*86400
```

```
4120 Z$=SEG(T$,11,2)
4130 T=T+VAL(Z$)*3600
4140 Z$=SEG(T$,14,2)
4150 T=T+VAL(Z$)*60
4160 Z$=SEG(T$,17,2)
4170 T=T+VAL(Z$)
4180 IF H=1 THEN 4220
4190 M$=T$
4200 H=1
4210 T0=T
4220 T=T-T0
4230 RETURN
4240 REM ********** THIS SUBROUTINE CREATES 2 AXIS ON SCREEN *********
4250 FOR I=1 TO 2
4260 VIEWPORT 3,130.4+47*(I=1),45+47*(I=1)
4270 WINDOW 0,X1*60,0,10
4280 AXIS 60/((X1)59)+1),1,0,0
4290 VIEWPORT 0,130.0+47*(I=1),45+47*(I=1)
4300 MOVE X1*60/2,0
4310 PRINT "TIME - PMT #";I;
4320 MOVE 0,6
4330 PRINT "VJRQJRLJRTJRS"
4340 NEXT I
4350 RETURN
4360 REM ***** SUBROUTINE: FINDS 2ND DEG. POLY. FINDS TIME AT MAXIMUM **
4370 IF I>5 AND I<=X6-4 THEN 4450
4380 IF I>5 THEN 4420
4390 Z7=A(1,1)-2*X2
4400 Z6=A(1,4)
4410 GO TO 4440
4420 Z7=0
4430 Z6=A(1,4)
4440 RETURN
4450 FOR I3=0 TO 4 STEP 4
4460 A2=0
```

```
4470 CALL "SETIP",1,I*4-19
4480 CALL "READ",1,A1
4490 FOR I2=1 TO 9
4500 Y(I2)=A1(I2,J*(I3=0)+I3)
4510 X(I2)=A1(I2,1)
4520 FOR J2=1 TO 3
4530 T3(J2)=X(I2)↑(J2-1)
4540 NEXT J2
4550 FOR J2=1 TO 3
4560 A2(J2,4)=T3(J2)*Y(I2)+A2(J2,4)
4570 FOR K2=1 TO 3
4580 A2(J2,K2)=T3(J2)*T3(K2)+A2(J2,K2)
4590 NEXT K2
4600 NEXT J2
4610 NEXT I2
4620 FOR I2=1 TO 3
4630 IF A2(I2,I2)=0 THEN 4750
4640 C3=A2(I2,I2)
4650 FOR J2=1 TO 4
4660 A2(I2,J2)=A2(I2,J2)/C3
4670 NEXT J2
4680 FOR J2=1 TO 3
4690 IF I2=J2 THEN 4740
4700 C3=A2(J2,I2)
4710 FOR K2=I2 TO 4
4720 A2(J2,K2)=A2(J2,K2)-C3*A2(I2,K2)
4730 NEXT K2
4740 NEXT J2
4750 NEXT I2
4760 IF I3=4 THEN 4780
4770 Z7=-(A2(2,4)/(2*A2(3,4)))
4780 NEXT I3
4790 Z6=A2(1,4)+A2(2,4)*Z7+A2(3,4)*Z7↑2
4800 RETURN
4810 REM ********** THIS SECTION LISTS UNPROCESSED DATA **********
```

```
4820 PRINT "↓INSERT TAPE CONTAINING UNPROCESSED DATA"
4830 PRINT "↓INPUT HEADER FILE NUMBER OF DATA: ";
4840 INPUT X3
4850 FIND X3
4860 GOSUB 3890
4870 PRINT "↓INPUT RANGE OF SCANS TO BE LISTED: MIN,MAX ";
4880 INPUT Z1,Z2
4890 IF Z1>0 THEN 4910
4900 Z1=1
4910 IF Z2<=X6 THEN 4930
4920 Z2=X6
4930 PRINT "↓HARD COPY? (Y/N) ";
4940 INPUT Z$
4950 FIND X3
4960 GOSUB 3890
4970 PRINT USING 4980:"SCAN#","TIME(SEC)","LOAD","PMT#1","PMT#2"
4980 IMAGE 3T,5A,13T,9A,31T,4A,48T,5A,65T,5A
4990 DIM B3(4)
5000 VIEWPORT 0,130,0,100
5010 C9=0
5020 J=0
5030 I=0
5040 FIND X3+1
5050 I=I+1
5060 ON EOF (0) THEN 5140
5070 READ @33:B3
5080 IF I<Z1 THEN 5050
5090 J=J+1
5100 PRINT USING 5110:I,B3(1),B3(4),B3(2),B3(3)
5110 IMAGE 5D,13D.1D,12D.4D,12D.4D,12D.4D
5120 IF J<30 AND I<Z2 THEN 5050
5130 C9=C9+1
5140 PRINT "↑↑↑↑↓                ";C9;"/";INT((Z2-Z1)/30+1)
5150 IF Z$="N" THEN 5190
5160 FOR K=1 TO 500
```

```
5170 NEXT K
5180 COPY
5190 IF I=>X6 OR I=>Z2 THEN 5240
5200 PRINT "LJJ"
5210 PRINT USING 4980:"SCAN#","TIME(SEC)","LOAD","PMT#1","PMT#2"
5220 J=0
5230 GO TO 5050
5240 MOVE 0,0
5250 PRINT "FINISHED: PRESS RETURN FOR MENU1";
5260 INPUT Z$
5270 GO TO 130
5280 REM ********** THIS SECTION LISTS PROCESSED DATA **************
5290 PRINT "JJINSERT TAPE CONTAINING PROCESSED DATA "
5300 PRINT "JINPUT HEADER FILE NUMBER OF DATA: ";
5310 INPUT X3
5320 PRINT "JHARD COPY? (Y/N) ";
5330 INPUT Z$
5340 FIND X3
5350 GOSUB 3890
5360 FIND X3+1
5370 PRINT "    TIME-1     LOAD     FIT-1     L-FIT    ";
5380 PRINT " TIME-2     LOAD     FIT-2     L-FIT ";
5390 DELETE B3
5400 VIEWPORT 0,130,0,100
5410 DIM B3(8)
5420 I=0
5430 J=0
5440 I=I+1
5450 J=J+1
5460 READ @33:B3
5470 PRINT USING 5480:B3(1),B3(2),B3(3),B3(4),B3(5),B3(6),B3(7),B3(8)
5480 IMAGE 8(6D.2D)
5490 IF J<30 AND I<X7*2 THEN 5440
5500 PRINT "↑JIII                    ";INT((I-1)/30+1);"/";INT((X7*2-1)/30+1);
5510 IF Z$="N" THEN 5560
```

```
5520 REM **** DELAY LOOP: LETS COPIER CATCH UP ****
5530 FOR K=1 TO 500
5540 NEXT K
5550 COPY
5560 IF I=X7*2 THEN 5620
5570 PRINT "LJ"
5580 PRINT "    TIME-1    LOAD    FIT-1    L-FIT   ";
5590 PRINT " TIME-2    LOAD    FIT-2    L-FIT ";
5600 J=0
5610 GO TO 5440
5620 MOVE 0,0
5630 PRINT "FINISHED: PRESS RETURN FOR MENU1"
5640 INPUT Z$
5650 GO TO 130
5660 REM ********** THIS SECTION PLOTS UNPROCESSED DATA **************
5670 DIM B3(4),B4(4)
5680 PRINT "LINSERT TAPE CONTAINING DATA TO BE PLOTTED"
5690 PRINT "JINPUT HEADER FILE NUMBER OF DATA: ";
5700 INPUT X3
5710 FIND X3
5720 GOSUB 3890
5730 PRINT "JPLOT ALL OR PART OF DATA (A OR P,0=QUIT): ";
5740 INPUT Z$
5750 Z1=0
5760 Z2=X1
5770 IF Z$="0" THEN 130
5780 IF Z$="A" THEN 5850
5790 PRINT "JINPUT TIME RANGE (MINUTES:MIN,MAX): ";
5800 INPUT Z1,Z2
5810 IF Z1>0 THEN 5830
5820 Z1=0
5830 IF Z2<=X1 THEN 5850
5840 Z2=X1
5850 FIND X3
5860 GOSUB 3890
```

```
5870 X1=Z2-Z1
5880 GOSUB 4240
5890 WINDOW Z1*60,Z2*60,0,10
5900 MOVE Z1*60,0
5910 PRINT Z1;
5920 MOVE Z2*60,0
5930 PRINT "ΔΔΔΔΔΔ";Z2;
5940 FIND X3+1
5950 I2=0
5960 ON EOF (0) THEN 6130
5970 READ @33:B3
5980 IF B3(1)<Z1*60 THEN 5970
5990 IF B3(1)>Z2*60 THEN 6130
6000 B3(4)=B3(4)*8
6010 IF I2=0 THEN 6100
6020 VIEWPORT 3,130,51,92
6030 MOVE ABS(B4(1)),ABS(B4(2))
6040 DRAW ABS(B3(1)),ABS(B3(2))
6050 VIEWPORT 3,130,4.45
6060 MOVE ABS(B4(1)),ABS(B4(3))
6070 DRAW ABS(B3(1)),ABS(B3(3))
6080 MOVE ABS(B4(1)),ABS(B4(4))
6090 DRAW ABS(B3(1)),ABS(B3(4))
6100 I2=1
6110 B4=B3
6120 GO TO 5970
6130 PRINT "↑"
6140 INPUT Z$
6150 GO TO 5710
6160 REM ***** THIS SECTION PLOTS PROCESSED DATA *****
6170 DELETE B3
6180 DIM B3(8)
6190 PRINT "LINSERT TAPE CONTAINING DATA TO BE PLOTTED "
6200 PRINT "JINPUT HEADER FILE NUMBER OF DATA: ";
6210 INPUT X3
```

```
6220 FIND X3
6230 GOSUB 3890
6240 FOR I=1 TO 10
6250 CALL "OPEN",I+50,1,8
6260 CALL "KILL",I+50
6270 CALL "OPEN",I+50,1,8
6280 NEXT I
6290 FIND X3+1
6300 FOR I=0.5 TO X7 STEP 0.5
6310 CALL "WRITE",51,I
6320 CALL "WRITE",56,I
6330 READ @33:B3
6340 FOR J=1 TO 4
6350 CALL "WRITE",51+J,B3(J)
6360 CALL "WRITE",56+J,B3(J+4)
6370 NEXT J
6380 NEXT I
6390 PRINT "JJIPLOTTING OPTIONS:"
6400 PRINT "JI          MAIN MENU        (0)"
6410 PRINT "I         DISPLACEMENT     (1)"
6420 PRINT "I         TIME (MAX/MIN)   (2)"
6430 PRINT "I         LOAD (MAX/MIN)   (3)"
6440 PRINT "I         FIT TIME         (4)"
6450 PRINT "I         FIT LOAD         (5)"
6460 PRINT "JCHOOSE X-AXIS PARAMETER (0-5): ";
6470 INPUT M1
6480 IF M1=0 THEN 7300
6490 PRINT "JCHOOSE Y-AXIS PARAMETER (0-5): ";
6500 INPUT M2
6510 IF M2=0 THEN 7300
6520 IF M1=M2 THEN 6460
6530 PRINT "JWHICH PMT DATA TO BE PLOTTED (1,2,OR 3=BOTH): ";
6540 INPUT Z
6550 CALL "MAX1",M1+50,M5,M9
6560 CALL "MAX1",M2+50,M6,M9
```

```
6570 CALL "MAX1",M1+55,M7,M9
6580 CALL "MAX1",M2+55,M8,M9
6590 M3=M5 MAX M7
6600 M4=M6 MAX M8
6610 GO TO M1 OF 6620,6650,6700,6750,6770
6620 Q$="DISPLACEMENT"
6630 M5=1
6640 GO TO 6790
6650 Q$="TIME"
6660 M5=60
6670 IF M3/M5<59 THEN 6690
6680 M5=3600
6690 GO TO 6790
6700 Q$="LOAD"
6710 M5=10
6720 IF M3/M5<50 THEN 6740
6730 M5=100
6740 GO TO 6790
6750 Q$="FIT TIME"
6760 GO TO 6660
6770 Q$="FIT LOAD"
6780 GO TO 6710
6790 GO TO M2 OF 6800,6830,6880,6930,6950
6800 S$="D_I_S_P_L_A_C_E_M_E_N_T"
6810 M6=1
6820 GO TO 6970
6830 S$="T_I_M_E"
6840 M6=60
6850 IF M4/M6<60 THEN 6870
6860 M6=3600
6870 GO TO 6970
6880 S$="L_O_A_D"
6890 M6=10
6900 IF M4/M6<50 THEN 6920
6910 M6=100
```

```
6920 GO TO 6970
6930 S$="F_I_T_ _T_I_M_E"
6940 GO TO 6840
6950 S$="F_I_T_ _L_O_A_D"
6960 GO TO 6890
6970 FIND X3
6980 GOSUB 3890
6990 VIEWPORT 3,130,4,92
7000 WINDOW 0,M3,0,M4
7010 AXIS M5,M6,0,0
7020 VIEWPORT 0,130,0,92
7030 MOVE M3/2-M3/7,0
7040 IF Z=3 THEN 7070
7050 PRINT Q$;"  PMT#";Z;
7060 GO TO 7080
7070 PRINT Q$;"  PMT#1 AND #2";
7080 MOVE 0,M4/2
7090 PRINT S$;
7100 VIEWPORT 3,130,4,92
7110 FOR I=1 TO 10
7120 CALL "SETIP",I+50,1
7130 NEXT I
7140 FOR M0=50+5*(Z=2) TO 55-5*(Z=1) STEP 5
7150 CALL "READ",M1+M0,M7
7160 CALL "READ",M2+M0,M8
7170 MOVE M7,M8
7180 FOR I=1 TO X7 STEP 0.5
7190 CALL "READ",M1+M0,M7
7200 CALL "READ",M2+M0,M8
7210 DRAW M7,M8
7220 NEXT I
7230 IF Z<>3 OR (Z=3 AND M0=55) THEN 7250
7240 PRINT "HH#1";
7250 NEXT M0
7260 PRINT "I"
```

```
7270 INPUT Z$
7280 PAGE
7290 GO TO 6390
7300 FOR I=1 TO 10
7310 CALL "KILL",50+I
7320 NEXT I
7330 DELETE M0,M1,M2,M3,M4,M5,M6,M7,M8,M9
7340 GO TO 130
7350 REM ***** THIS SECTION TRANSFERS DATA TO PDP *****
7360 PRINT "LGGGGGGTERMINAL MODE FOR DATA TRANSFER GGGGGJ"
7370 PRINT "JJYOU MUST :"
7380 PRINT "      1. TYPE...LOGIN (RETURN)"
7390 PRINT "      2. TYPE...CREATE filename  (RETURN)"
7400 PRINT "      3. PRESS MENU"
7410 PRINT "      5. FOLLOW INSTRUCTIONS"
7420 GOSUB 7900
7430 PRINT "LJTRANSFER UNPROCESSED OR PROCESSED DATA (1 OR 2) ";
7440 INPUT W
7450 PRINT "JINSERT DATA TAPE CONTAINING DATA TO BE TRANSFERRED "
7460 PRINT "JENTER HEADER FILE NUMBER OF DATA: ";
7470 INPUT F
7480 FIND F
7490 GOSUB 3890
7500 PRINT "JJDATA BEING TRANSFERRED - DO NOT INTERRUPT"
7505 PRINT @40,30:
7510 FIND F+1
7520 PRINT @40:C$;"  LENGTH:";X1;" (MIN)  LOAD CAL:";X8
7525 INPUT @40:A$
7530 PRINT @40:"#SCANS:";X6;"   PERIOD:";X2;"   HEADER FILE#:";X3;"   ";
7540 PRINT @40:X7;"  FRINGES"
7545 INPUT @40:A$
7550 PRINT @40:"GAIN:";X4;"/";X5;"   ";G$;"   START:";E$;"   STOP:";F$
7555 INPUT @40:A$
7560 GO TO W OF 7580,7650
7570 GO TO 7430
```

```
7580 PRINT @40:"TIME/VOLTS-PMT#1/VOLTS-PMT#2/LOAD(LBS)"
7585 INPUT @40:A$
7590 DELETE B3
7600 DIM B3(4)
7610 ON EOF (0) THEN 7780
7620 READ @33:B3
7630 PRINT @40:B3(1),B3(2),B3(3),B3(4)
7635 INPUT @40:B3(1),B3(2),B3(3),B3(4)
7640 GO TO 7620
7650 DELETE B3
7660 DIM B3(8)
7670 FOR I=1 TO 5 STEP 4
7680 PRINT @40:"FRINGE#/TIME/LOAD/T-FIT/L-FIT"
7685 INPUT @40:A$
7690 FIND F+1
7700 S9=0
7710 ON EOF (0) THEN 7760
7720 READ @33:B3
7730 S9=S9+0.5
7740 PRINT @40:S9;B3(I);B3(I+1);B3(I+2);B3(I+3)
7745 INPUT @40:S9,B3(I),B3(I+1),B3(I+2),B3(I+3)
7750 GO TO 7720
7760 PRINT @40:-999;-999;-999;-999;-999
7765 INPUT @40:B3(1),B3(2),B3(3),B3(4)
7770 NEXT I
7780 PRINT @40:"Z"
7790 FOR J=1 TO 500
7800 NEXT J
7810 PRINT "JGGGGGFILE TRANSFERRED AND CLOSED"
7811 PRINT "JDO YOU WANT TO LOGOFF? (Y/N) ";
7812 INPUT Z$
7813 IF Z$="N" THEN 7830
7814 PRINT @40:"LO"
7815 PRINT "JTEK LOGGED-OFF PDP"
7830 PRINT "JJPRESS RETURN FOR MENU I";
```

```
7840 INPUT Z$
7850 GO TO 130
7860 REM ***** THIS SUBROUTINE INTERFACES TO PDP (TERMINAL MODE) *****
7870 PRINT "LJTERMINAL MODE  (PRESS MENU TO EXIT)JJ"
7880 GOSUB 7900
7881 PAGE
7890 GO TO 7811
7900 CALL "CMSET"
7910 CALL "MARGIN",0,0,0
7920 CALL "RATE",1200,5,1
7930 CALL "TERMIN"
7940 RETURN
7950 REM ***** THIS SECTION CALLS K CALC. ROUTINE FROM AUX. MEMORY *****
7960 CALL "MSHUE",100,"L.J. DATA AQU."
7970 CALL "MLINK",101,100
7980 REM ***** DUMMY LINE FROM AUTO LOAD PROCEEDURE *****
```

AD-A189 846 FRACTURE TOUGHNESS TESTING OF A CERAMIC MATRIX COMPOSITE(U) AIR FORCE INST OF TECH WRIGHT-PATTERSON AFB OH SCHOOL OF ENGINEERING R P VOZZOLA DEC 87 2/2

UNCLASSIFIED AFIT/GAE/AA/87D-24 F/G 11/2 NL

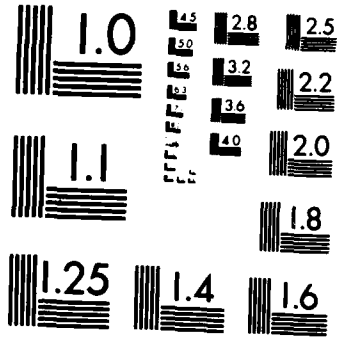

Bibiliqraphy

1. Griffith, A.A. "The Theory of Rupture and Flow in Solids," Phil. Trans. Roy. Soc. of London, A221: 163-197 (1921).

2. Griffith, A.A. "The Theory of Rupture," Proc. 1st Int. Conqress Apppl. Mech., (1924): 55-63. Biezeno and Burgers ed. Waltman, (1925).

3. Irwin, G.R. "Fracture dynamics," Fracturinq of Metals: 147-166, ASM publ. (1948).

4. Broek, David. Elementary Engineering Fracture Mechanics (Third Revised Edition). The Hague: Martinus Nijhoff Pub. (1986).

5. Jones, Robert M. Mechanics of Composite Materials. New York: Hemisphere Publishing Corporation (1975).

6. Lamicq, P.J., Bernhardt, G.A., Daucher, M.N., Mace, J.G., "SiC/SiC Laminar Composite," American Ceramic Society Bulletin, V65: 336-338 (1986).

7. Prewo, Karl M. "The Development of Fiber Reinforced Glasses and Glass Ceramics," Proceedinqs of the Conference Tailoring Multipurpose and Composite Ceramics, Penn State, July, 1985.

8. Prewo, K.M., Thompson, E.R. "Research on Graphite Reinforced Glass Matrix Composites," NASA Contractor Report 159312, Feb. 1980.

9. Prewo, K.M., Thompson, E.R. Research on Graphite Reinforced Glass Matrix Compostes, NASA Contractor Report 165711, May 1981.

10. ASTM Standard E399-78A, "Standard Test Method for Plane-Strain Fracture Toughness of Metallic Materials," 1979 Annual Book of ASTM Standards, Part 10: 540-561 (1979): Philadelphia.

11. Jenkins, M.G., Kobayash, A.S., Saka, M., White, K.W., Bradt, R.C. "Fracture Toughness Testinng of Ceramics Using a Laser Interferometric Strain Gage," submitted to the American Ceramic Society Bulletin, June 1986.

12. Jenkins, M.G. Ceramic Crack Growth Resistance Determination Utilizing Laser Interferometry. PhD dissertation. University of Washington, Seattle, Washington, 1987.

13. Sharpe, William N. Jr. "Interferometric Surface Strain Measurement," International Journal of Nondestructive Testing, Vol. 3: 59-76. (1981).

14. Sharpe, W.N., Jr. and Grandt, A.F., Jr. A Laser Interfero-metric Technique for Crack Surface Displacement Measurement. Air Force Material Laboratories, AFML - TR-74-75, July 1974.

15. Macha, D.E., Sharpe, W.N. Jr., and Grandt, A.F., Jr. A Laser Intermetry Method for Experimental Stress Intensity Factor Calibration, Cracks and Fracture. ASTM TP 606, American Society for Testing and Materials, 1976, p. 490-505.

16. Sharpe, W.N. Jr., and Grandt, A.F., Jr. A Preliminary Study of Fatique Crack Retradation Using Laser Interferometry to Measure Crack Surface Displacement, Mechanics of Crack Growth. ASTM STP 590. American Society for Testing and Materials, 1976, 302-320.

17. Russell, A.J. "Factors Affecting the Interlaminar Fracture Energy of Graphite/Epoxy Laminants," Progress in Science and Engineering of Composites, Proceedings of ICMM-IV, Tokyo, Japan, 1982, 279-286.

18. Mall, S. and Kochhar, N.K. "Finite-Element Analysis of End-Notch Flexure Specimens." Journal of Composites Technology & Research, Vol. 8, No. 2, Summer 1986: 54-75.

19. Giare, G.S. "Fracture Toughness of Unidirectional Fiber Reinforced Composites in Mode II," Engineering Fracture Mechanics, Vol. 20, No. 1: 11-21 (1984).

20. Jelinek, F.J. "Ceramic Composites," Batelle's Metals and Ceramic Information Center under DOD sponsorship.

21. "Processing Techniques for Fiber-Reinforced Ceramic Matrix Composites," Ceramic Bulletin, Vol. 65, No. 2: 297-304 (1986).

22. Rice, R.W. and others, "Refractory-Ceramic-Fiber Composites: Progress, Needs and Opportunities," Proceedings of the 6th Anual Conference on Composites and Advanced Ceramic Materials: 698-713. Columbus; The American Ceramic Society (1982).

23. Hasselman, D.P.H. "Elastic Energy at Fracture and Surface Energy as Design Criteria for Thermal Shock," Journal of the American Ceramic Society, 46 (11): 535-540 (November 1963).

24. Hasselman, D.P.H. "Crack Propagation Under Constant Deformation and Thermal Stress Fracture," International Journal of Fracture Mechanics, 7 (2): 157-161 (June 1971).

25. Hasselman, D.P.H. "Thermal Stress Resistance Parameters for Brittle Refractory Ceramics: A Compendium," American Ceramic Society Bulletin, 49 (12): 1033-1037 (December 1970).

26. Kelly, William H., II. Thermal Shock Resistance of Mullite-Based SiC - Whisker Composites. MS Thesis, AFIT/GAE/AA/86D-6, School of Engineering, Air Force Institute of Technology (AU), Wright-Patterson AFB OH, December 1986.

27. Valentine, Peter G. Strength and Thermal Shock Resistance of SiC - BN Composites. MS Thesis, AFIT/GAE/AA/83D-27, School of Engineering, Air Force Institute of Technology (AU), Wright-Patterson AFB OH, December 1983.

28. Prewo, K.M. "Silicon Carbide Yarn of New Composites," Composites Review: 69-71.

29. Prewo, K.M., Brennan, J.J. "Silicon Carbide Fiber Reinforced Glass-Ceramic Matrix Composite Exhibiting High Strength and Toughness," Journal of Materials Science 17: 2371-2383 (1982).

30. Prewo, K.M., Brennan, J.J., "Silicon Carbide Yarn Reinforced Glass Matrix Composites'" Journal of Materials Science 17: 1201-1206 (1982).

31. Prewo, K.M. "A compliant, High Failure Strain, Fiber-Reinforced Glass Matrix Composite," Journal of Materials Science 17: 3549-3563 (1982).

32. Strife, J.R., Prewo, K.M. "Silicon Carbide Fiber-Reinforced Resinn Matrix Composites," Journal of Materials Science 17: 65-72 (1982).

33. Prewo, K.M., Brennan, J.J. "High Strength Silicon Carbide Fiber Reinforced Glass-Matrix Composites," Journal of Materials Science 15: 463-468 (1980).

34. Prewo, K.M., Brennan, J.J., Layden, G.K. "Fiber Reinforced Glasses and Glass-Ceramics for High Performance Applications," Ceramic Bulletin, Vol 65, No. 2: 305-313 (1986).

35. Prewo, K.M. "Fiber Reinforced Metal and Glass Matrix Composites," Presented at the Distinguished Lecture Series "Frontiers in Materials Science," Sandia National Labs, Oct. 1983.

36. Prewo, K.M., Minford, E.J. "Graphite Fiber Reinforced Thermoplastic Glass Matrix Composites for Use at 1000°F," Proceedings of the Sixteenth Nationnal Sampe Conference, Albequerque, NM, Oct. 1984.

37. Zawada, L.P., ceramic engineer, Metals and Ceramic Division. Personal interviews. AFWAL/MLLN, Wright-Patterson AFB, Ohio, 2 June - 6 Nov. 1987.

38. ASTM Standard Practice E561-81, "Standard Practice for R-Curve Determination," 1982 Annual Book of ASTM Standards, Part 10: 680-699 (1982): Philadelphia.

39. ASTM Standard D790-84a, "Standard Test Methods for Flexural Properties of Unreinforced and Reinforced Plastics and Electical Insulating Materials," 1985 Annual Book of ASTM Standards, Section 8: 397-409 (1985): Philadelphia.

40. Kobayashi, Albert S. Experimental Techniques in Fracture Mechanics. Ames, Iowa: The Iowa State University Press and Westport Connecticut: Society for Experimental Stress Analysis, 1973.

41. Kobayashi, Albert S. Experimental Techniques in Fracture Mechanics, 2. Ames, Iowa: The Iowa State University Press and Westport, Connecticut: Society for Experimental Stress Analysis, 1975.

42. Ramulu, M. and Jenkins, M.G. "A Notched Specimen for Short Fatigue Crack," To be published in Experimental Technology.

43. Jenkins, M.G. and others, "Crack Initiationn and Arrest in a SiC Whisker/Al_2O_3 Matrix Composite," To be published in American Ceramic Society Bulletin.

44. Sukere, A.A. and Sharpe, W.N., Jr. "Transient Response of a Central Crack to a Tensile Pulse," Experimental Mechanics: 89-98 (March 1983).

45. Sharpe, W.N. and Martin, D.R. "Optical Measurement of In-Plane Strainn/Displacement Near Crack Tips at High Temperatures" Unknown.

46. Sharpe, W.N. and Mendonhall, F. "Preliminary Measurements in Aluminum Graphite-Epoxy Composite Test Specimens," College of Engineering, Michigan State University.

47. Sharpe, W.N., Jr. and Moss, G.L. "Dynamic Measurement of CTOD," Proceedings of the Nineteenth National Symposium on Fracture Mechanics, Philadelphia: ASTM, 1986.

48. Sharpe, W.N., Jr. Development and Applicationn of an Interferometric System for Measuring Crack Displacements, 1 March 1975 - 30 June 1976. Grant NSG 1148. Division of Engineering Research, Michigan State University, East Lansing, Michigan.

49. Bar-Tikva, D. An Experimental Weight Function Method for Stress Intensity Factor Calibration. MS thesis, AFIT/GAE/AA/79D-2. School of Engineering, Air Force Institute of Technology (AU), Wright-Patterson AFB, Ohio, December 1979.

50. Bar-Tikva, D., Grandt, A.F., Jr., Palazotto, A.N. "An Experimental Weight Function for Stress-intensity-factor Calibrations," Experimental Mechanics, vol. 21, No. 10: 371-378 (1981).

51. Jira, J. Test Engineer. Personal interviews. AFWAL/MLLN, Wright-Patterson AFB, Ohio, 1 July 1987 - 6 November 1987.

52. Wiederhorn, S.M. "Brittle Fracture and Toughnening Mechanics in Ceramics," Annual Review of Material Science 14: 373-403 (1984).

54. Lankford, James, Jr. "Characterization of Mechanical Damage Mechanisms in Ceramic Composite Materials," ONR Contract No. N00014-84-C-0213, June 1985.

55. Marshall, D.B. and Evans, A.G. "Failure Mechanisms in Ceramic-Fiber/Ceramic-Matrix Composites," Journal of the American Ceramic Society, Vol. 68, No. 5: 225-231 (1985).

VITA

Captain Robert P. Vozzola was born on 7 March 1958 in Hartford, Connecticut. He graduated from high school in Windsor Locks, Connecticut, in 1976 and attended the Worcester Polytechnic Institute of Massachusetts, from which he received the degree of Bachelor of Science in Mechanical Engineering in May 1980. Upon graduation, he received a commission in the USAF through the ROTC program. He was employed as a process engineer, for Reddington Counters, Inc., Windsor, Connecticut, until called to active duty in March 1981. He served as a project engineer and branch chief for the 4501st Computer Services Squadron and the 1912th Information Systems Support Group, Langley, AFB, Virginia until entering the School of Engineering, Air Force Institute of Technology, in May 1986.

Permanent address: 180 Taft Lane
Windsor Locks
Connecticut 06096

UNCLASSIFIED
SECURITY CLASSIFICATION OF THIS PAGE

A184 546

REPORT DOCUMENTATION PAGE

Form Approved
OMB No. 0704-0188

1a. REPORT SECURITY CLASSIFICATION UNCLASSIFIED	1b. RESTRICTIVE MARKINGS
2a. SECURITY CLASSIFICATION AUTHORITY	3. DISTRIBUTION / AVAILABILITY OF REPORT Approved for public release; distribution unlimited
2b. DECLASSIFICATION / DOWNGRADING SCHEDULE	
4. PERFORMING ORGANIZATION REPORT NUMBER(S) AFIT/GAE/AA/87D-24	5. MONITORING ORGANIZATION REPORT NUMBER(S)
6a. NAME OF PERFORMING ORGANIZATION School of Engineering 6b. OFFICE SYMBOL (If applicable) AFIT/ENY	7a. NAME OF MONITORING ORGANIZATION
6c. ADDRESS (City, State, and ZIP Code) Air Force Institute of Technology Wright-Patterson AFB OH 45433-6583	7b. ADDRESS (City, State, and ZIP Code)
8a. NAME OF FUNDING / SPONSORING ORGANIZATION Metals & Ceramics Division 8b. OFFICE SYMBOL (If applicable) AFWAL/MLLN	9. PROCUREMENT INSTRUMENT IDENTIFICATION NUMBER
8c. ADDRESS (City, State, and ZIP Code) AFWAL/MLLN Wright-Patterson AFB OH 45433	10 SOURCE OF FUNDING NUMBERS PROGRAM ELEMENT NO. / PROJECT NO. / TASK NO / WORK UNIT ACCESSION NO.

11. TITLE (Include Security Classification)
FRACTURE TOUGHNESS TESTING OF A CERAMIC MATRIX COMPOSITE

12. PERSONAL AUTHOR(S)
Robert P. Vozzola, Capt, USAF

13a. TYPE OF REPORT	13b. TIME COVERED	14. DATE OF REPORT (Year, Month, Day)	15. PAGE COUNT
MS Thesis	FROM _____ TO _____	1987 December	95

16. SUPPLEMENTARY NOTATION

17. COSATI CODES			18. SUBJECT TERMS (Continue on reverse if necessary and identify by block number)
FIELD	GROUP	SUB-GROUP	Critical Strain Energy Release Rate, End-notch Flexure Specimen, Mode II, Laser Interferometric Strain Gauge

19. ABSTRACT (Continue on reverse if necessary and identify by block number)

Thesis Chairman: Dr. S. Mall
Professor of Aeronautical Engineering

Approved for public release: IAW AFR 190-1.
LYNN E. WOLAVER 31 Dec 87
Dean for Research and Professional Development
Air Force Institute of Technology (AFIT)
Wright-Patterson AFB OH 45433

20 DISTRIBUTION / AVAILABILITY OF ABSTRACT	21. ABSTRACT SECURITY CLASSIFICATION
☐ UNCLASSIFIED/UNLIMITED ☒ SAME AS RPT. ☐ DTIC USERS	UNCLASSIFIED
22a. NAME OF RESPONSIBLE INDIVIDUAL Dr. S. Mall	22b. TELEPHONE (Include Area Code) (513)-255-2362 / 22c. OFFICE SYMBOL AFIT/ENY

DD Form 1473, JUN 86 — Previous editions are obsolete. — SECURITY CLASSIFICATION OF THIS PAGE

UNCLASSIFIED

The need for an accurate fracture toughness testing technique for fiber reinforced ceramic composites was identified. A technique was developed to measure small crack mouth displacements over small gauge lengths of small glass-ceramic composite specimens during loading. The technique was applied to Mode II crack propagation. A loading fixture capable of exerting and measuring small loads was developed. A technique to measure compliances in small composite specimens was perfected. The validity of using a laser based interferometric technique to determine the instant of crack initiation was studied. Finally, the Mode II critical strain energy release rate of interlaminar delamination growth was evaluated. Sample results for a 1723 glass matrix, silicon carbide fiber composite are included and recommendations for further study are described.

END
DATE
FILM
4-88
DTIC